NMR Study of High Tc Superconductor : $Tl_2Ba_2CuO_{6+y}$

Kenji Fujiwara

OSAKA UNIVERSITY
GRADUATE SCHOOL OF ENGINEERING SCIENCE
DEPARTMENT OF MATERIAL PHYSICS
TOYONAKA OSAKA

Thesis

NMR Study of High Tc Superconductor : $Tl_2Ba_2CuO_{6+y}$

Kenji Fujiwara

Faculty of Engineering Science, Osaka University

February 1991

C O N T E N T S

ABSTRACT

$Tl_2Ba_2CuO_{6+y}$(Tl2201) is a typical material belonging to "heavy-doped" superconductor, and has many doping-holes in the CuO_2 plane. This compound shows a gradual transition from a 85 K superconductor to a nonsuperconducting normal metal, as excess oxygen content, y, is increased from 0 to 0.1. Three compounds (T_c=72, 40 and 0 K) were prepared. To study about static and dynamical properties of Cu-d spin in CuO_2 plane, Knight shift and nuclear relxation rate, $1/T_1$ for ^{63}Cu, were measured, and $1/T_1$ for ^{205}Tl was measured to obtain the information about Cu site indirectly.

In the normal state, $1/T_1$'s of ^{63}Cu for all compounds obey T_1T=const. law in a wide temperature range. This is the first observation of the T_1T=const. law of Cu in the CuO_2 plane. Applying the high magnetic field (= 11 T) along c-axis in superconducting compounds, T_c's decrease from 72 K and 40 K to 55 K and 20 K, respectively. Then $1/T_1$'s also obey T_1T=const. law above 55K and 20K, supporting that T_1T=const. law is an intrisic feature in Tl2201 compounds. As the T_1T=const. law means that the energy spectrum of Cu spin excitation is continuous, Fermi liquid picture is applicable to Tl2201 compounds. All $1/T_1$'s are enhanced much as that of Cu in the CuO_2 plane for $YBa_2Cu_3O_7$. The magnitude of $1/T_1$ does not change with hole concentration, in contrast to the result that $1/T_1$ of Cu for the "light-doped" La-Sr-Cu-O superconductor decreases considerably with increasing holes. This difference may be attributed to the differnce of

strength of Cu-d spin antiferromagnetic correlation between "heavy-doped" and "light-doped" superconductors.

In the superconductig states, temperature dependence of the spin susceptibility, χ_s estimated from spin contribution (K_s) to the Knight shift is explained by BCS model with a larger gap of $2\Delta = 4.4 K_B T_c$ than the BCS value of $2\Delta = 3.5 k_B T_c$. The behavior is similar to that for the CuO_2 plane in $YBa_2Cu_3O_7$. However, $1/T_1$ for ^{63}Cu decreases rapidly without the enhancement just below T_c predicted by the BCS model. The unconventional behavior is also observed for other several high T_c oxides, and all the $1/T_1$'s normalized by the value at $T=T_c$ plotted against T/T_c fall on a single curve, suggesting that the same mechanism is responsible for the relaxation process.

Chapter 1. Introdudtion

Since the discovery of high T_c superconductor by Bedonorz and Müller[1] in 1986, several kinds of high Tc materials (La·Sr·Cu·O, Y·Ba·Cu·O, Bi·Sr·Ca·Cu·O, Tl·Ba·Ca·Cu·O, Nd·Ce·Cu·O, ...) have been found out. A number of studies have been carried out in the world to elucidate the mechanism for "high T_c" superconductor. They have layered perovskite structure and planer CuO_2 layers. There is a general consensus that the presence of the CuO_2 layers and carriers doping are essential for the occurrence of the superconductivity. Well known phase diagram for the high T_c supercondoctors is shown in Fig. 1. Non-doped sample is an insulator and antiferromagnet caused by a super exchange interaction between Cu spins. With hole doping, the antiferromagnetic state is destroyed rapidly. With more hole doping, the superconducting state appears and then transforms to the metallic state.

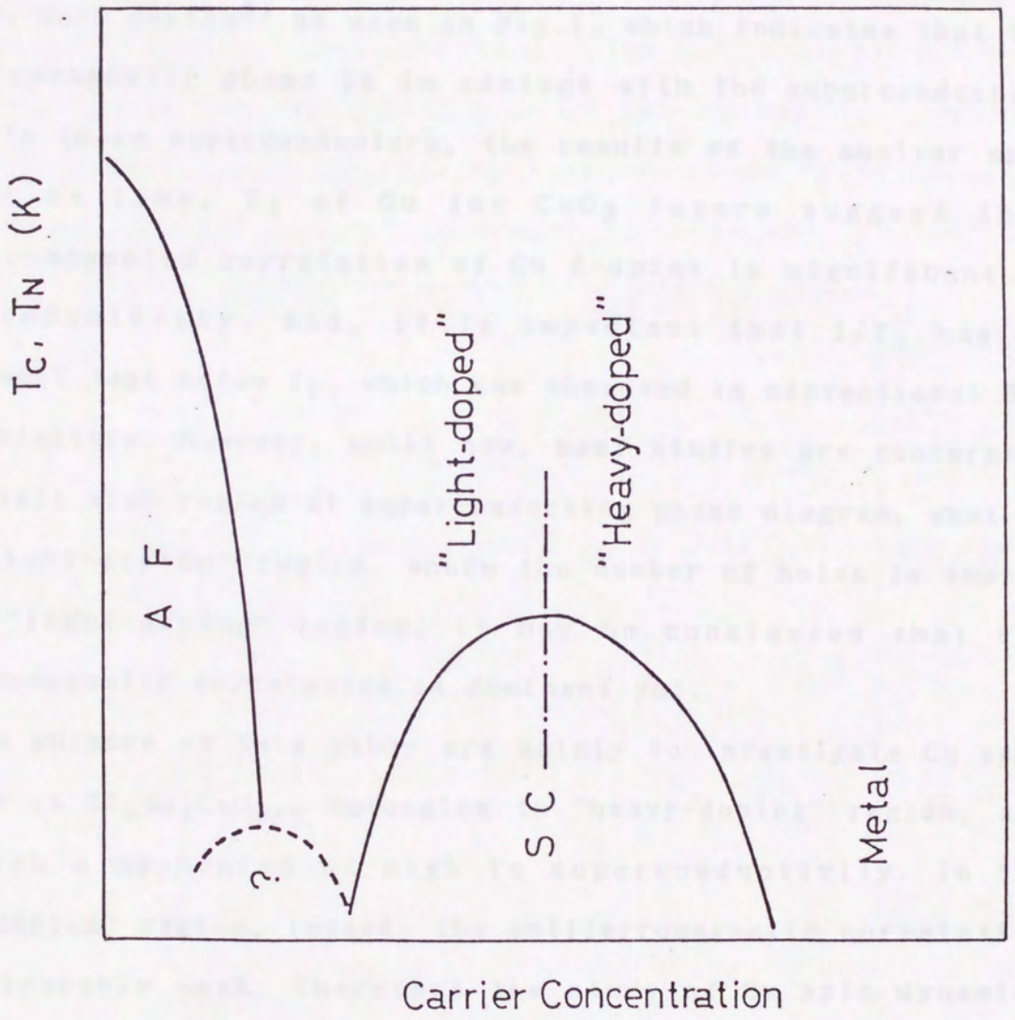

Fig. 1. Schematic phase diagram for the high Tc superconductor.

The nuclear magnetic resonance (NMR) has brought much significant information for the superconductivity. The NMR is powerful technique which provides information about the microscopic electronic state at each atomic site. For example, NMR contributes to determine phase diagrams of La-Sr-Cu-O system and Y-Ba-Cu-O system[2] as seen in Fig.1, which indicates that the antiferromagnetic phase is in contact with the superconducting phase. In these superconductors, the results of the nuclear spin relaxation time, T_1 of Cu for CuO_2 layers suggest that antiferromagnetic correlation of Cu d-spins is significant to superconductivity. And, it is important that $1/T_1$ has no enhancement just below T_c, which was observed in conventional BCS superconductors. However, until now, most studies are concerning to the left side region of superconducting phase diagram, what we call "light-doping" region, where the number of holes is small. In the "light-doping" region, it may be considered that the antiferromagnetic correlation is dominant yet.

The purpose of this study are mainly to investigate Cu spin dynamics in $Tl_2Ba_2CuO_{6+y}$ belonging to "heavy-doping" region, and to search a mechanism of high Tc superconductivity. In the "heavy-doping" region, indeed, the antiferromagnetic correlation is considerably weak. Therefore the study of Cu spin dynamics under such condition is significant itself. It is expected that this study gives some information whether the antiferromagnetic correlation is essential to superconductivity, or not.

Chapter-2. Superconductivity of $Tl_2Ba_2CuO_{6+y}$

It is noteworthy that $Tl_2Ba_2CuO_{6+y}$ (2201 compound) is a typical high T_c superconductor in "Heavy-doping" region, and that this compound shows a gradual transition from a 85 K superconductor to a nonsuperconducting normal metal, as excess oxygen content, y is increased from 0 to 0.1.(see Fig.2) The excess oxygens were controlled by the annealing temperture.[3] Recently, good quality samples have been made by Shimakawa et.al. and the features of 2201-compounds as below are revealed by their works.[3)-6)]

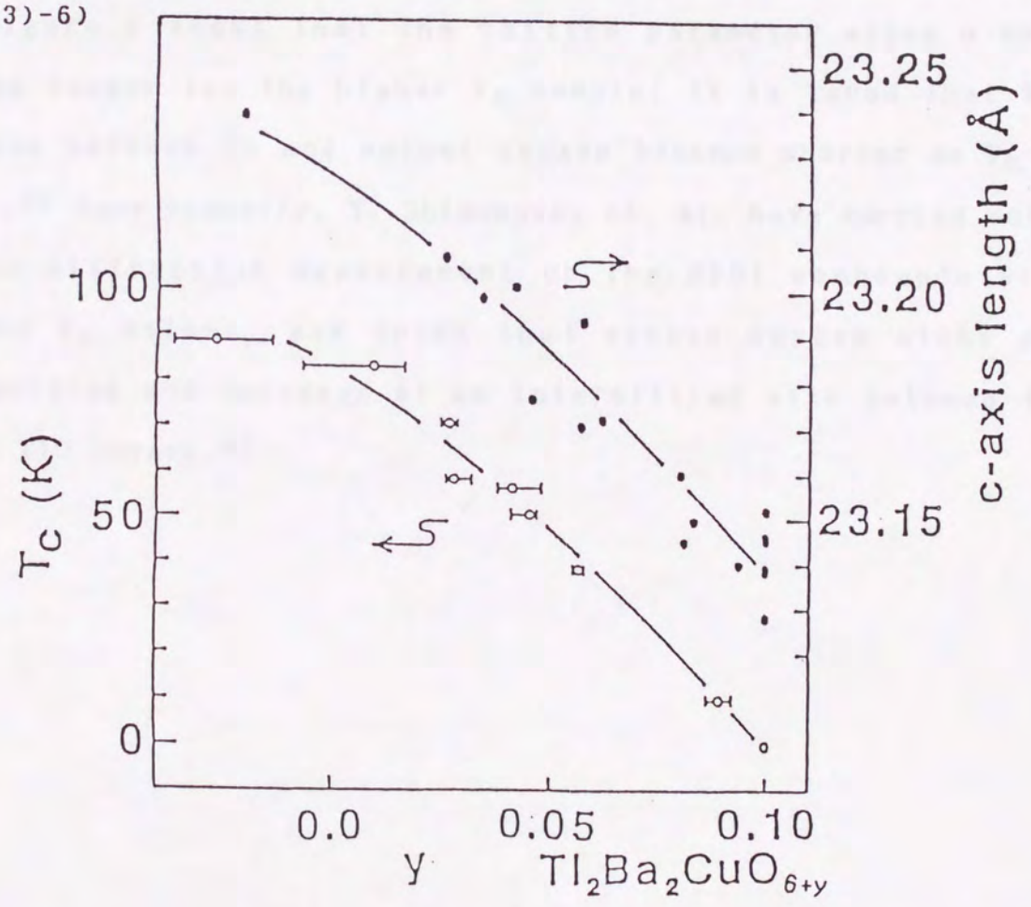

Fig. 2. Tc values and c-axis lengths plotted against the relative change in the oxygen content in $Tl_2Ba_2CuO_6$.

2-1. Structure

As seen in Fig. 3, the 2201 compounds have single CuO_2 plane, where Cu is surrounded by octahedral oxygens like the LaSrCuO system. Both Cu and Tl atoms have single site crystallographically. For 2201 compounds, two structures, namely, tetragonal and orthorhombic, were reported.[3] However, there is no differnce in physical properties between these structures. Our samples have tetragonal structure and perfect single phase.

Figure 2 shows that the lattice parameter along c axis becomes longer for the higher T_c sample. It is found that the distance between Cu and apical oxygen becomes shorter as T_c is higher.[4] Very recently, Y. Shimakawa, et. al. have carried out a neutron diffraction measurement on the 2201 compounds with various T_c values, and found that excess oxygen atoms are incorpolated and released at an interstitial site between the double TlO layers.[5]

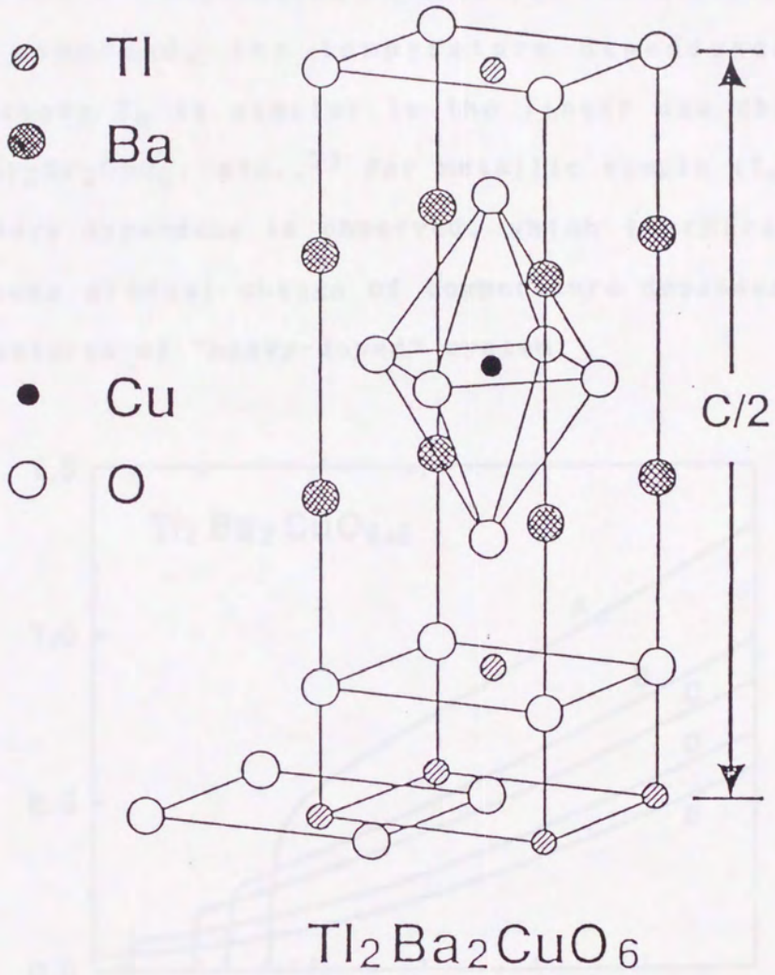

Fig. 3. Crystal structure of $Tl_2Ba_2CuO_{6+y}$.

2-2. Transport Properties

Electric Resistivity[4),6)]

Figure 4 shows T dependence of electric resistivity. For the highest T_c compound, the temperature dependence of the resistivity above T_c is similar to the linear one observed in $YBa_2Cu_3O_7$, $Bi_2Sr_2CuO_6$, etc..[7)] For metallic sample (T_c=0 K), T^2 like temperature dependece is observed, which is characteristic of metal. These gradual change of temperature dependence may be one of the features of "heavy-doped" system.

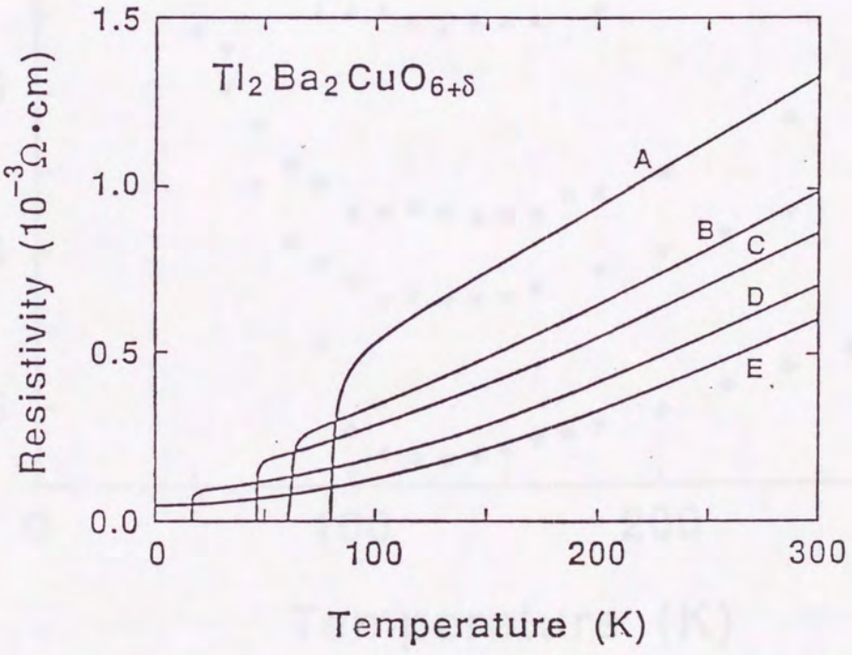

Fig. 4. The temperature dependence of the resistivity for $Tl_2Ba_2CuO_{6+y}$ with various T_c's. (T_c's of sample A-E are 81, 62, 47, 16 and 0 K, respectively.)

Hall Effect[6)]

Figure 5 shows T dependence of the hole number. As Hall coefficient is positive and decreases with increasing excess oxygen content, y, in $Tl_2Ba_2CuO_{6+y}$, origin of hole doping is attributed to the excess oxygen. The hole number increases gradually with decreasing from T_c= 85 k to 0 K.

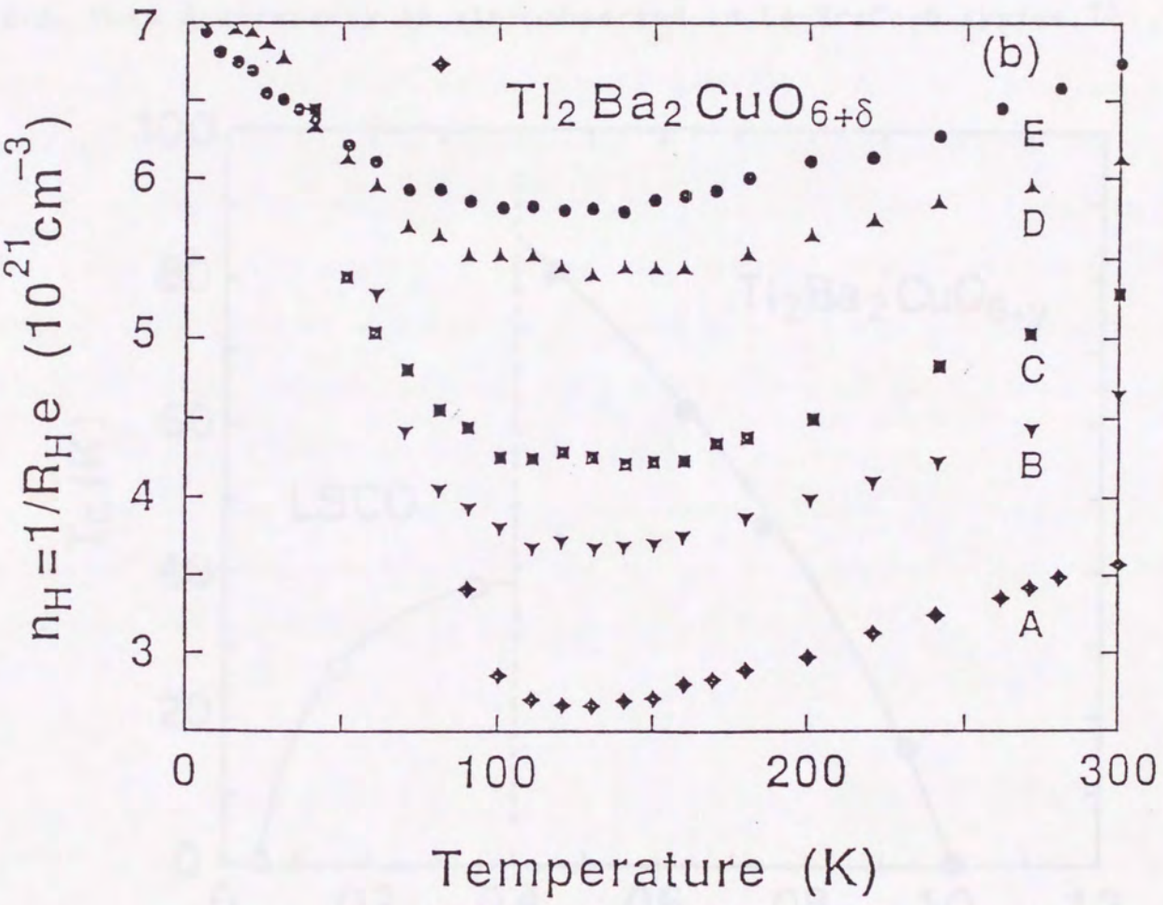

Fig. 5. The temperature dependence of the Hall number for $Tl_2Ba_2CuO_{6+y}$ with various T_c's.

In Fig. 6, T_c is plotted against the hole number per Cu for $Tl_2Ba_2CuO_{6+y}$ and $(La_{1-x}Sr_x)_2CuO_4$.[7] It is convincing that 2201 compounds belong to "heavy-doping" region. However, the change of the hole number between the highest T_c and metallic samples is about 0.5. On the other hand, the change of the excess oxygens between both samples is about 0.1. As excess oxygen creates two holes per Cu, the expected change of the hole number change is 0.2. This discrepancy is also observed in La-Sr-Cu-O system.[7]

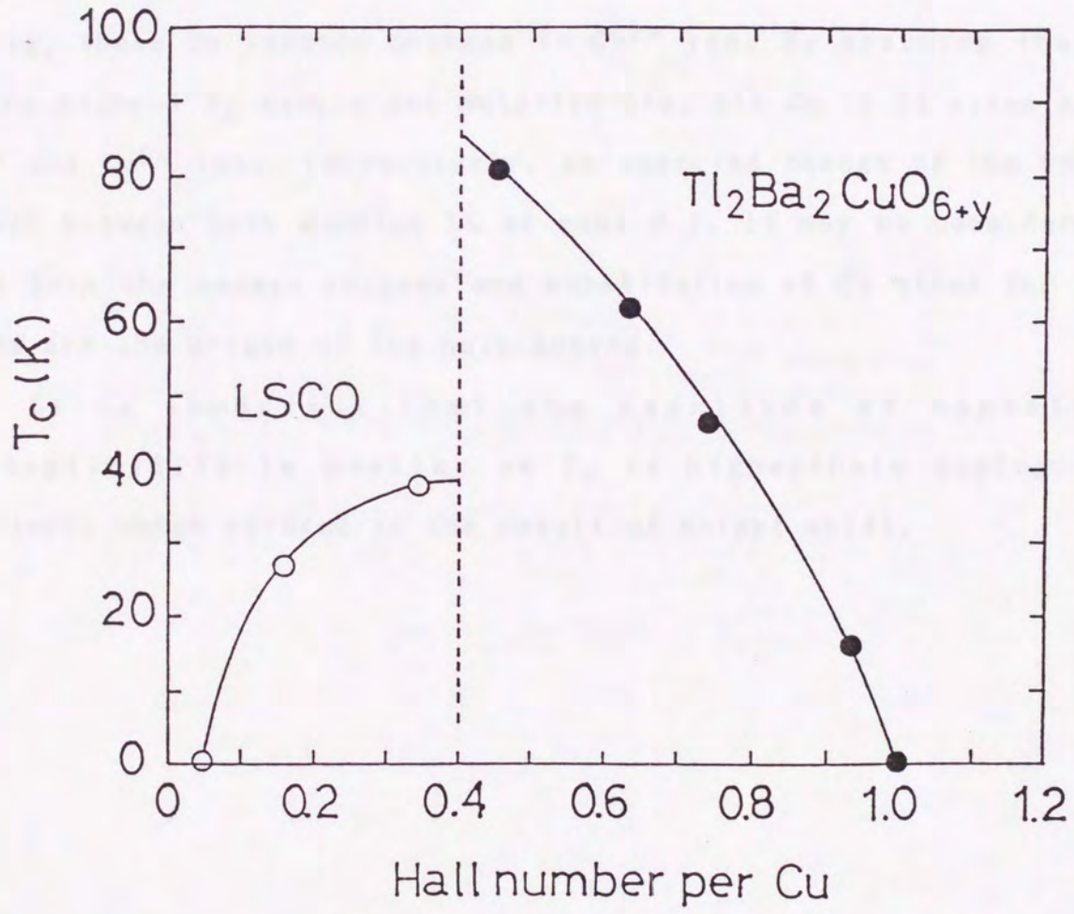

Fig. 6. Relationship between T_c and the hole number per Cu for $Tl_2Ba_2CuO_{6+y}$ and $(La_{1-x}Sr_x)_2CuO_4$.

2-3. Magnetic Susceptibility[6)]

As seen in Fig. 7, the magnetic susceptibility shows Curie like temperature dependence, and the Curie term becomes small with increasing Tc. Shimakawa et.al. speculate that the Curie term dose not result from impurity of extra phases, but Cu^{2+} ions substituted for the Tl site. Actually, their Rietveld analysis of X-ray diffraction suggests that 3-5% of Tl sites are replaced by Cu atoms. They also consider that Cu atoms in Tl sites prefer to exist as Cu^{1+} ion with no magnetic moment, and that, with hole doping, these Cu valence changes to Cu^{2+} ion. By assuming that, in the highest T_c sample and metallic one, all Cu in Tl sites are Cu^{1+} and Cu^{2+} ions, respectively, an expected change of the hole number between both samples is at most 0.1. It may be considered that both the excess oxygens and substitution of Cu atoms for Tl sites are the origin of the hole doping.

It is important that the magnitude of magnetic susceptibility is smaller as T_c is higher(hole doping is smaller), which relates to the result of Knight shift.

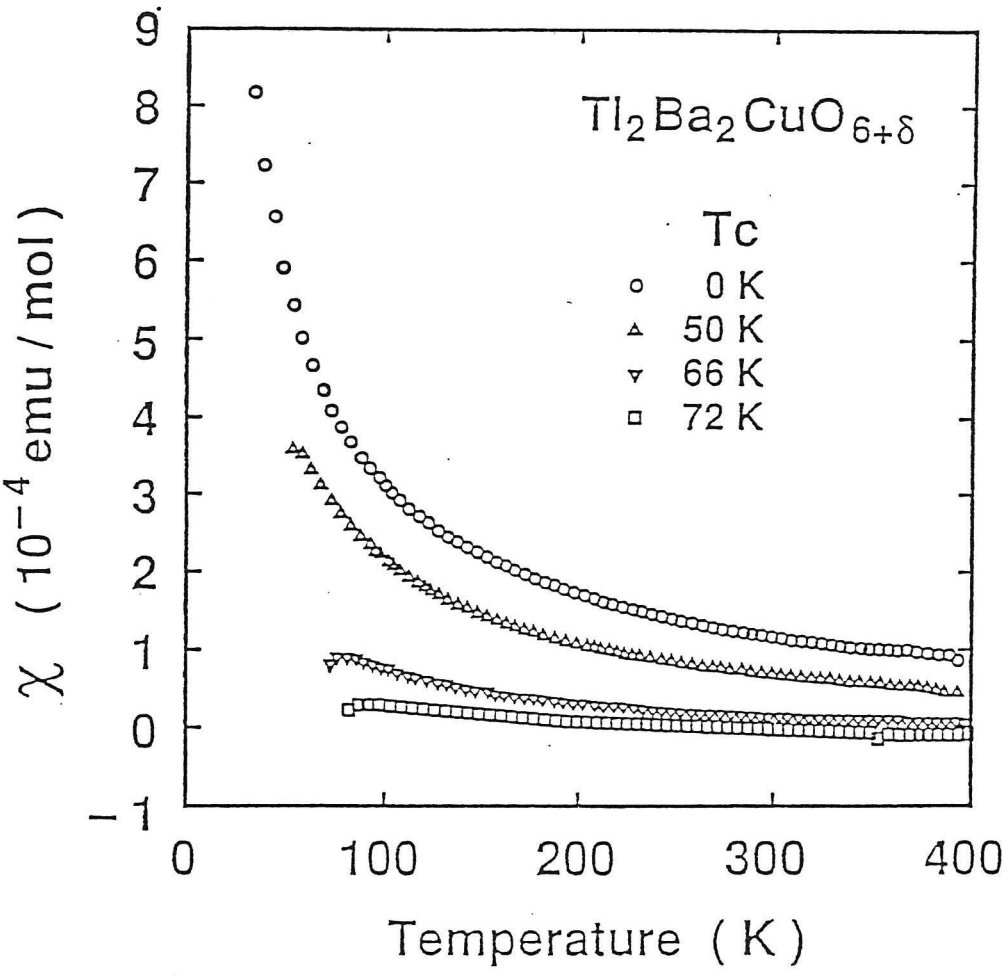

Fig. 7. The temperature dependence of the total measured magnetic susceptibility for $Tl_2Ba_2CuO_{6+y}$ with various T_c's.

Chapter-3. NMR Theory

In this chapter, the temperature dependence of the Knight shift and nuclear relaxation rate, $1/T_1$, in a conventional BCS superconductor are reviewed.

3-1 Knight Shift

In non-transition metal like aluminum, the hyperfine field mainly attributed to Fermi contact interaction with conduction electrons. Then the Knight shift is proportional to the Pauli spin susceptibility, χ_n. Under the external static field, H_0, the spin magnetization, M_S, is expressed by the formula,

$$M_S = \mu_B(n_\uparrow - n_\downarrow)$$

$$= \mu_B \sum_k \{ f(\varepsilon_k - \mu_B H_0) - f(\varepsilon_k + \mu_B H_0) \}$$

$$\sim -2\mu_B^2 H_0 \sum_k df/d\varepsilon_k, \qquad (3\text{-}1)$$

where $f(\varepsilon_k)$ is the Fermi-Dirac distribution function for a electron of energy ε_k, and μ_B is the Bohr magneton. Thus,

$$\chi_n = M_S/H_0 = -2\mu_B^2 \sum_k df/d\varepsilon_k. \qquad (3\text{-}2)$$

In superconducting state, Cooper pairs formed by up and down-spins do not contribute to the spin susceptibility, χ_s. Since only excited quasi-particles contribute to χ_s, the expression of χ_s is

$$\chi_s = -2\mu_B^2 \sum_k df/dE_k, \qquad (3\text{-}3)$$

where E_K is the energy of excited states. In BCS scheme, the energy density of excited states, N_S is given by

$$N_S(E) = N_0 \cdot |E| / (E^2 - \Delta^2)^{1/2}, \qquad (3\text{-}4)$$

where N_0 and Δ are the density of states (in the norml state) at the Fermi level and the T-dependent energy gap parameter, respectively. The sum in eq.(3-3) is replaced by an integral.

$$\chi_s = -4\mu_B^2 \int_\Delta^\infty N_S(E)(df/dE)dE. \qquad (3\text{-}5)$$

This result was calculated by Yosida[8], and consistent with that of Knight shift for alminum[9], as seen in Fig. 8.

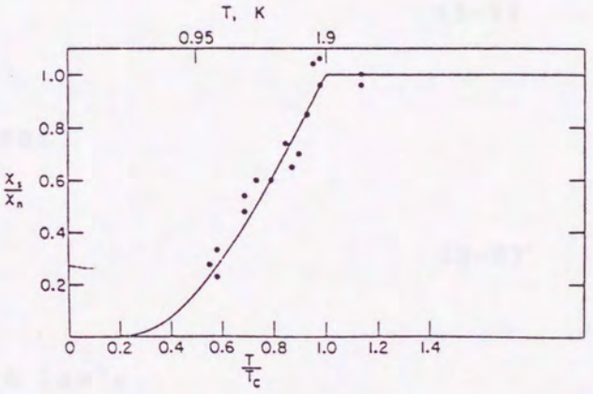

Fig. 8. Spin susceptibility in superconducting aluminum

3-2 Nuclear Relaxation Rate

Normal State

The expression of $1/T_1$, associated with the Fermi contact interaction , is given by

$$1/T_1 \propto \int N^2(E) f(E) \{1-f(E)\} dE, \qquad (3\text{-}6)$$

where N(E) is the density of states of the conduction electrons. Since $f(E)\{1-f(E)\}$ is nearly equal to $k_B T \delta (E-E_F)$, the eq.(3-6) yields

$$1/T_1 \propto k_B T N^2(E_F), \qquad (3\text{-}7)$$

where E_F is the Fermi energy. Then,

$$1/(T_1 T) \propto N^2(E_F) = \text{const.} \qquad (3\text{-}8)$$

This relation is called "Korringa law".

Superconducting State

In the superconducting state, $1/T_1$ is given by

$$1/T_1 \propto \int \{ N_s^2(E) + M_s^2(E) \} f(E) \{1-f(E)\} dE, \qquad (3\text{-}9)$$

where $N_s(E)$ is given by the eq.(3-4), and what is called the "anormalous" density of states, $M_s(E)$, is given by

$$M_S(E) = N_0 \Delta / (E^2 - \Delta^2)^{1/2}. \qquad (3\text{-}10)$$

Ms relate to "coherence effect". Since both M_S and N_S diverge at E Δ, as seen in Fig. 9, $1/T_1$ is enhanced just below T_c. At low temperture ($T \ll T_c$), f(E) is nearly exponential and therefore $1/T_1$ also decreases exponentially with the T-decrease. The behavior of $1/T_1$ for ^{27}Al in the superconducting alminum[9),10)] is consistent with that calculated with using above eq.(3-9), as seen in Fig. 10.

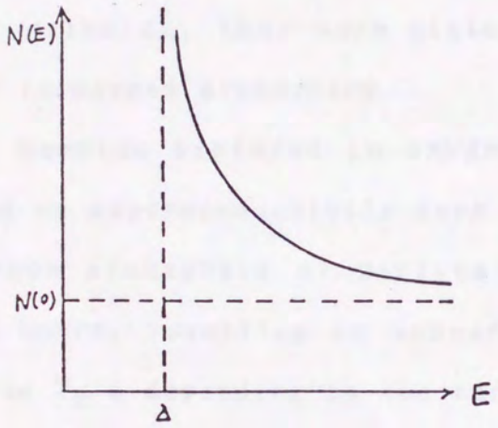

Fig. 9. BCS density of states

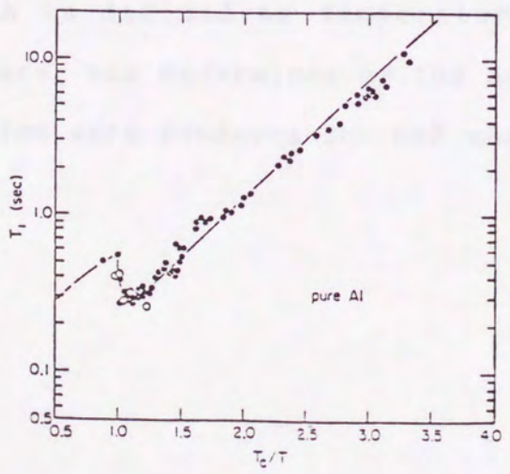

Fig.10.

Dependence of ^{27}Al relaxation time on T_c/T in superconducting aluminum. The solid line is calculated with the eq.(3-9).

Chapter 4. Experimental Procedure

4-1. Sample Preparation[4)]

Single phase polycrystalline samples of $Tl_2Ba_2CuO_{6+y}$ were prepared by solid state reactions. Mixtures of Tl_2O_3, BaO and CuO powders were pressed into pellets. The pellets were wrapped in Au foil, and sintered at 860 °C for 5-10 hours in oxygen atomsphere. After grinding, they were sintered again at 880-890 °C for 5-10 hours in oxygen atomsphere.

Samples sintered in oxygen atomsphere were metallic and showed no superconductivity down to 10 K. They were then annealed in argon atomsphere at various temperatures ranging 300-590 °C for 5 hours, resulting in appearance of superconductivity with various T_c's depending on the annealing temperature. In this way, three samples(T_c = 0, 40, 72 K) were obtained. X-ray diffraction did not show any impurity phases for all samples. T_c, which is defined as temperature where the diamagnetic signal appears, was determined by the ac susceptibility measurement. All samples were powdered for NMR measurement.

4-2. Cryostat

^{63}Cu and ^{205}Tl NMR measurement were performed in the high field (H = 10-11 T) between T=4.2 K and 300 K. For ^{63}Cu, NQR measurement in the zero field was performed.

High Field Cryostat

High field NMR of ^{63}Cu and ^{205}Tl were performed in a cryostat shown in Fig. 11. The cryostat enables us to control temperature between 1.3-400 K and apply field up to 12 tesla. The sample was set at the center of the superconducting magnet. The temperature was monitored by Pt thin film thermometor and carbon glass thermometor. Inhomogeneity of magnetic field at the center of the magnet is less than 10^{-5} Thus, the precise measurement of the Knight shift is practicable.

NQR Cryostat

As seen in Fig. 12, NQR cryostat has a simple structure, since ^{63}Cu NQR measurement was carried out in zero field and does not need the magnet. Sample's temperature is controlled by two heaters. The upper heater is used to warm the sample and the lower heater is used to cool down by evaporating ^{4}He liquid. The temperature is monitored by the thermocouple thermometor.

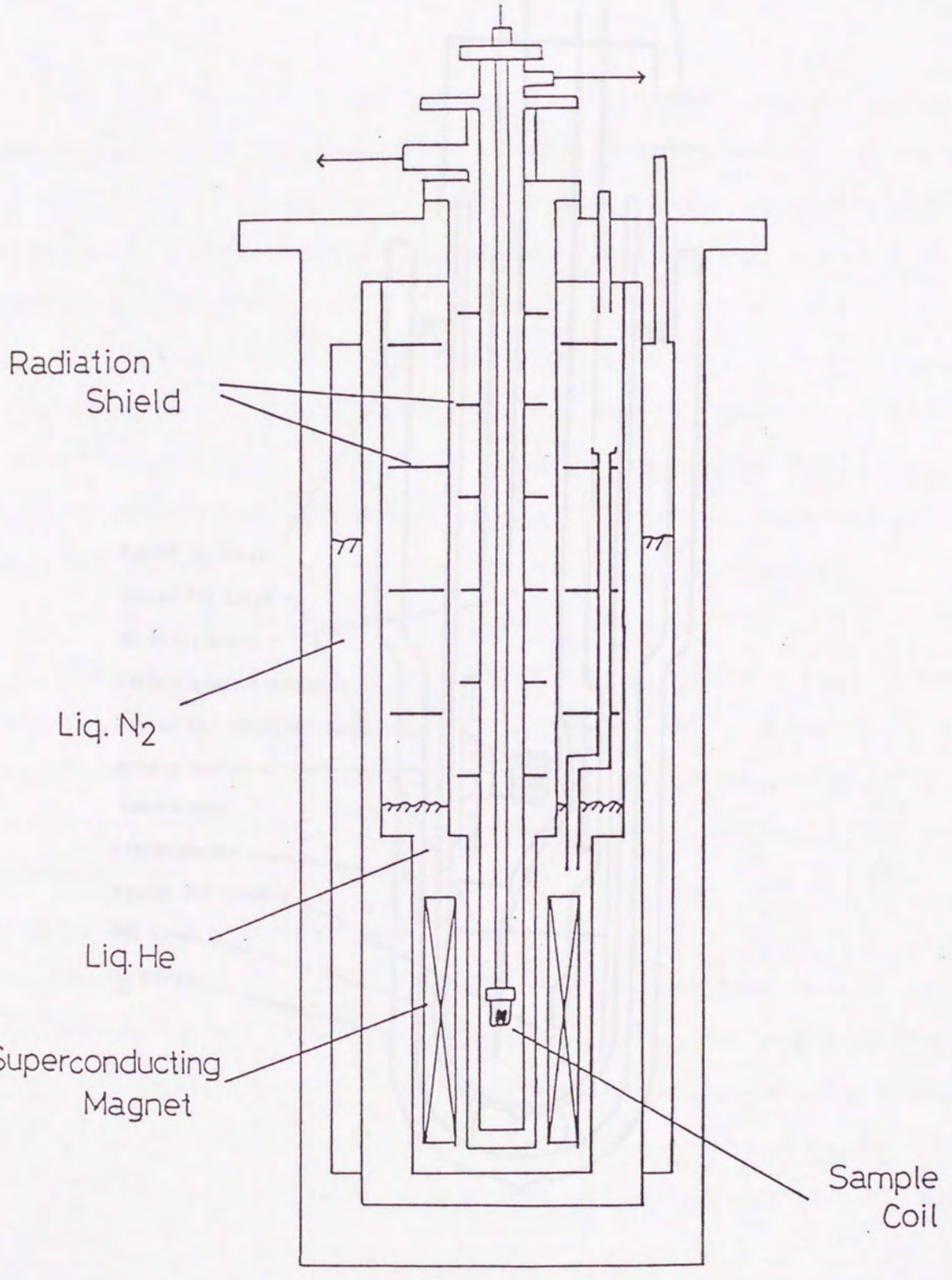

Fig.11. Cryostat for the high field NMR.

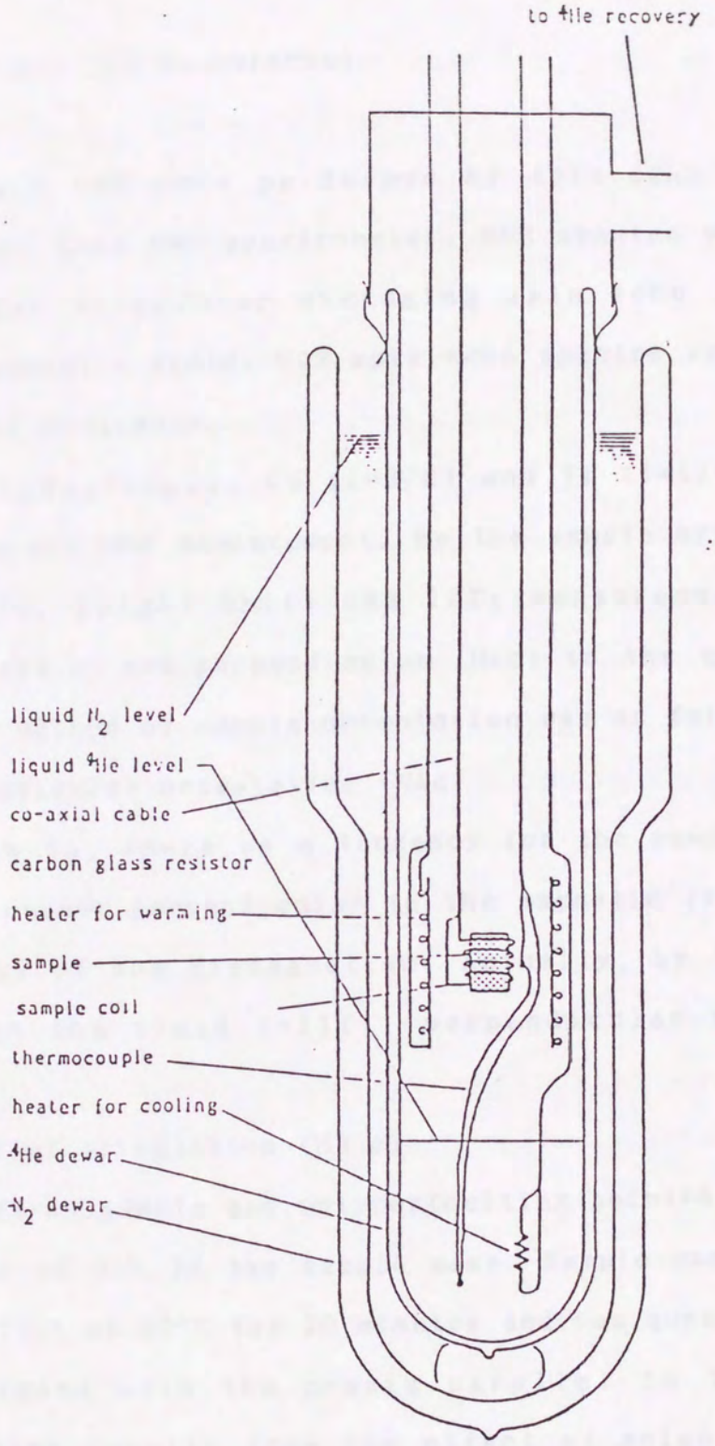

Fig.12. Cryostat for Cu NQR.

4-3. NMR and NQR Measurement

NMR and NQR were performed by spin echo method using a conventional type NMR spectrometer. NMR spectra were obtained by the Box Car Integrator averaging spin echo intensity with sweeping magnetic field. NQR spin echo spectra were plotted as a function of frequency.

In $Tl_2Ba_2CuO_{6+y}$, Cu (I=3/2) and Tl (I=1/2) nucleus were observable for NMR measurement. By the sample orientation in the high field, Knight Shift and $1/T_1$ measurement in the field parallel ($H \parallel c$) and parpendicular ($H \perp c$) to the c-axis have been made. The method of sample orientation was as follows,

1) perpendicular orientation ($H \perp c$)

Below T_c, there is a tendency for the powder to be aligned with the c-axis perpendicular to the magnetic field owing to the anisotropy of the diamagnetism. Actually, by the vibration of sample in the field (=11T), perpendicular orientation was achieved.

2) parallel orientation ($H \parallel c$)

Powdered sample and polymer(melting point=60K) were mixed at the ratio of 4:1 in the sample case. Sample case was put in the field (=11T) at 80°C for 20 minutes and was quenched. The powders were aligned with the c-axis parallel to the field. This orientation results from the effect of anisotropy of Cu spin susceptibility.

For both methods of orientation, the orientation was not perfect. This is due to the fact that the each powder particle was not a

single crystal. However, both orientations were enough to perform the precise measurements of Knight shift and T_1.

In order to determine the quadrupolar and Knight shifts for Cu separately, series of spectra were taken at several frequencies in the range of 110-130 MHz.

Saturation method was used for measurement of T_1. A $\pi/2$ pulse was applied to satulate nuclear magnetization. After the time, t, $\pi/2$-π pulse series were applied to observe spin echo. Since intensity of spin echo is in proportion to the magnetization recovered after t, decay of magnetization is obtained by changing t. T_1 measurement of Cu was performed in the central peak of the quadrupolar split line. Then, the magnetization; M(t) at t obeys the following equation,

$$M(t) = M_0 \left(1 - 0.9 \exp\left(\frac{-6t}{T_1}\right) - 0.1 \exp\left(\frac{-t}{T_1}\right)\right) \qquad (4\text{-}1)$$

where M_0 is a thermal equilibrium magnetization. As seen in Fig.17, T_1 was obtained by a least square fitting to above equation in the recovery of magnetization observed.

As Cu nucleus has I=3/2 and quadrupole moment, NQR was observable. NQR measurement in the zero field has great advantage on studying about superconductivity. NQR spectra and T_1 for each sample were measured.

Chapter 5. Experimental Results

In $Tl_2Ba_2CuO_{6+y}$ belonging to "heavy-doped" system, Knight shift and T_1 for ^{63}Cu and ^{205}Tl were measured to investigate normal and superconducting properties. Results of Knight shift and $1/T_1$ of ^{63}Cu were described in Sec.1 and Sec.2-3, respectively. Results of $1/T_1$ of ^{205}Tl were described in Sec.4.

5-1. Knight shift of ^{63}Cu

In order to study the intrinsic properties in the normal and the superconducting states in series of $Tl_2Ba_2CuO_{6+y}$ which have a simple structure like $La_{2-x}Sr_xCuO_4$, we have carried out a 63Cu high-field Knight shift measurement up to 11.5 T for three compounds with T_c=72 K, T_c=40 K and T_c=0 . Here T_c in the magnetic field of 11.5 T was determined as the temperature where the Knight shift starts to decrease. The polycrystalline samples were prepared by a conventional powder method described elsewhere.[4] The Cu NMR spectrum was obtained by sweeping the magnetic field in a frequency range of 110 MHz -130 MHz from 4.2 K to 150 K.

Fig. 13 (a) and (b) show the ^{63}Cu NMR spectrum in the partially oriented powder, with the c-axis parallel and perpendicular to the magnetic field, respectively, at 4.2 K and 125.02 MHz for the compound with T_c=72 K. The spectrum comes from the (1/2)-(-1/2) transition affected by the second order quadrupole effect. Although the orientation is not perfect, enhancement of NMR intensity by orientation is enough to determine the Knight shift precisely.

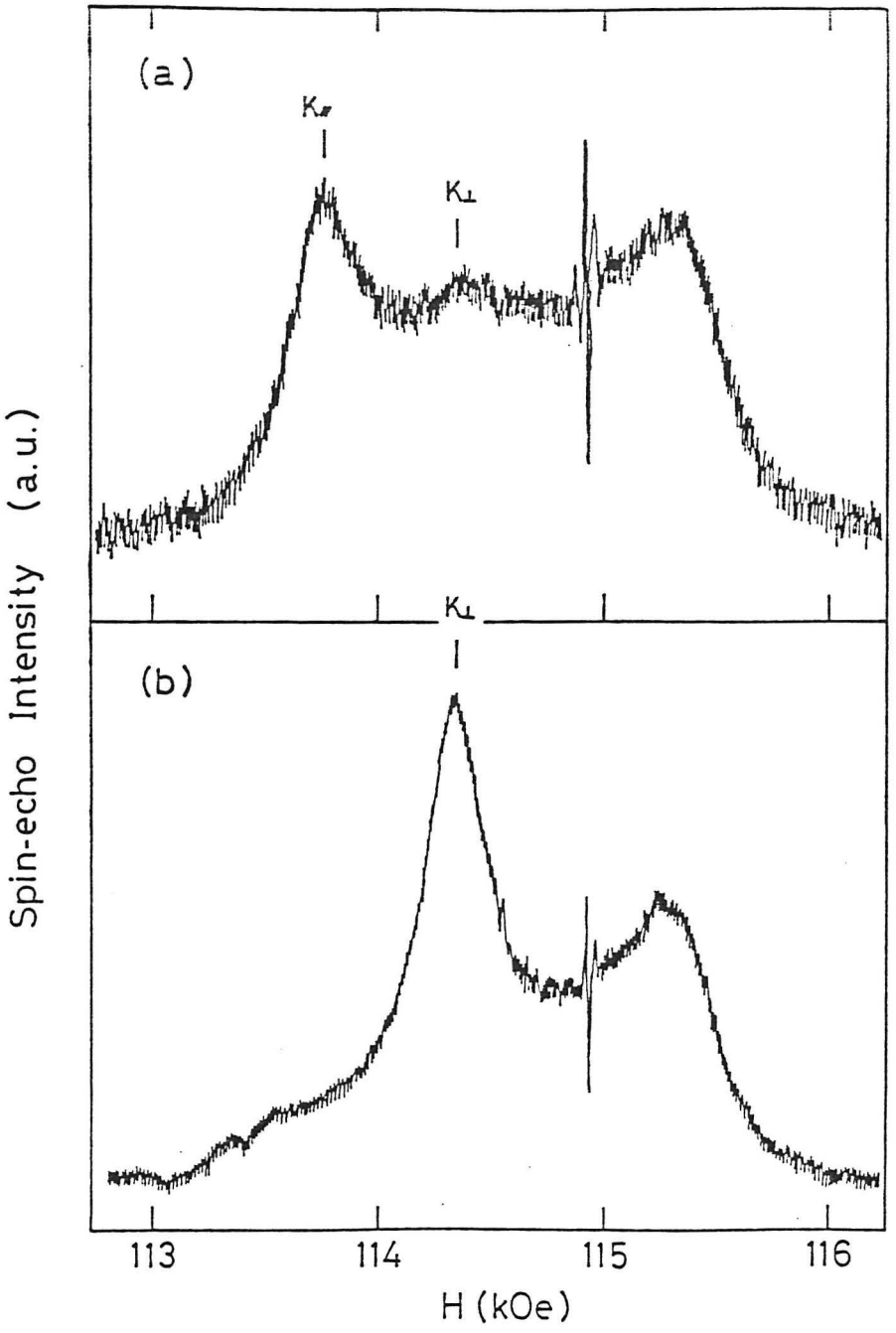

Fig.13. ^{63}Cu NMR spectra of $Tl_2Ba_2CuO_{6+y}$ with T_c=72 K obtained by sweeping the magnetic field at 125.02 MHz. (a) and (b) correspond to the spectra for the powder samples with partially oriented in parallel and perpendicular to the external field, respectively.

In order to determine the quadrupolar and the Knight shift separately, the series of spectra were taken at several different frequencies between 110 and 130 MHz. Following the same procedure as in $YBa_2Cu_3O_7$[12], where the value of $(\omega_0 - {}^{63}\gamma_N H_{res}(\theta))/{}^{63}\gamma_N H_{res}(\theta)$ are plotted against $({}^{63}\gamma_N H_{res}(\theta))^2$, a nice linear relation was obtained, as seen in Fig. 14 (a)-(c). Here ω_0 is the resonance frequency, $H_{res}(\theta)$ is the field corresponding to the peak of NMR intensity in Fig. 13 (a) and (b), and ${}^{63}\gamma_N$ the nuclear gyromagnetic ratio. In $Tl_2Ba_2CuO_{6+y}$, each sample has axial symmetry and its principal axis of the electric field gradient is c-axis. In this case, the shift along c-axis has no quadrupolar shift, and therefore has constant value independent of the frequency. Then the Knight shift K and the second order quadrupole shift have been evaluated from the intercept and the slope of these lines, respectively. In these analyses, we neglect the higher order quadrupolar shift, $\Delta\nu$ which is estimated as $\Delta\nu/{}^{63}\gamma_N H_{res} < 0.7\times10^{-4}$, because there is an experimental error of +0.01 % for the determination of the shift. Thus obtained $K_\perp$ and $K_\parallel$ for the compounds with T_c= 72 K, 40 K and 0 K are shown as closed and open circles in Fig. 15 (a)-(c), respectively.

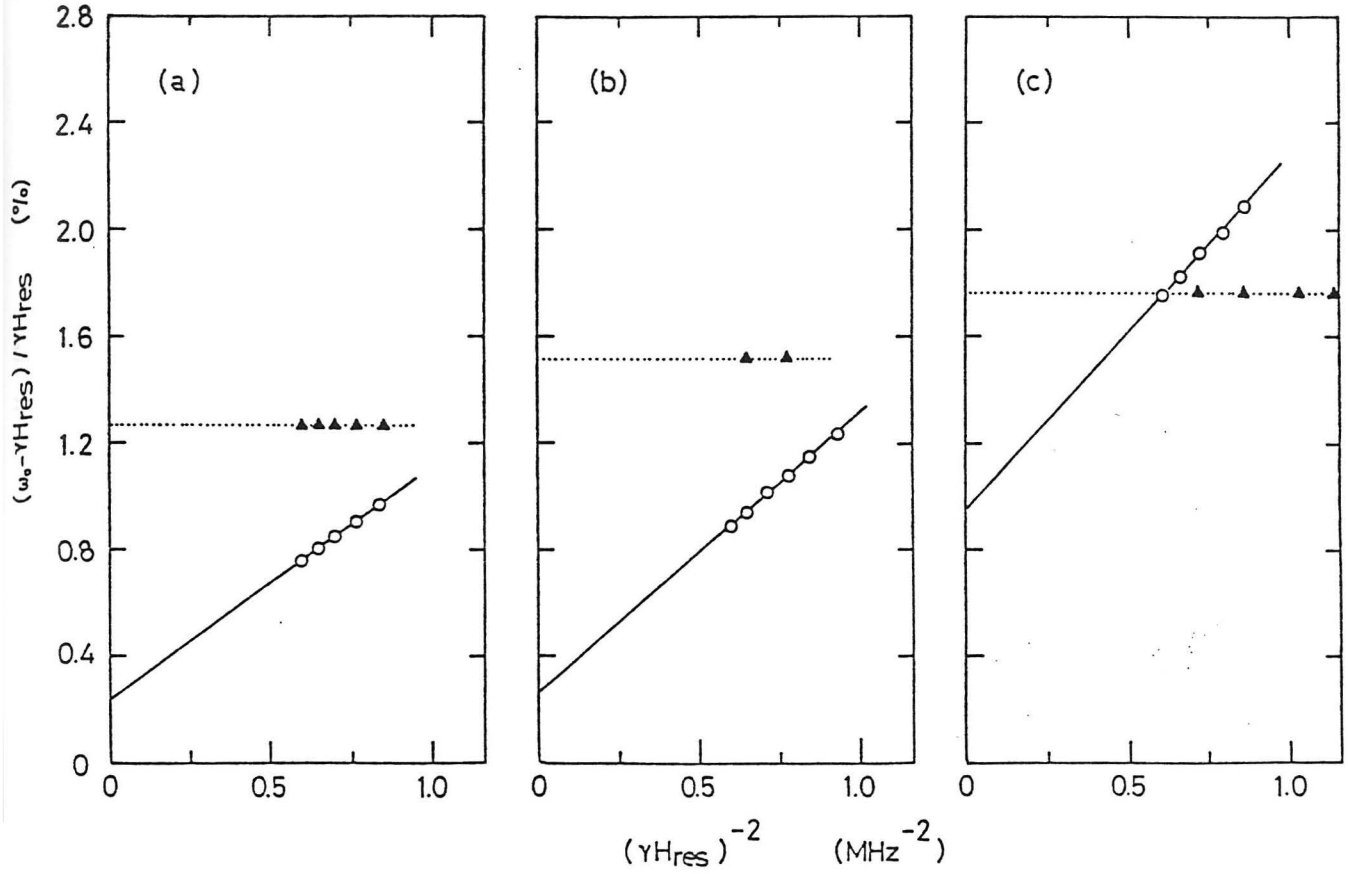

Fig.14. The value of $\{\omega_0-{}^{63}\gamma_N H_{res}(\theta)\}/{}^{63}\gamma_N H_{res}(\theta)$ is plotted against $\{{}^{63}\gamma_N H_{res}(\theta)\}^2$ for (a): T_c=72K, (b); T_c=40K and (c); T_c=0 K. Here ω_0 is the resonance frequency, $H_{res}(\theta)$ is the field corresponding to the peak of NMR intensity in Fig.15 (a) and (b), θ is the angle between the direction of external field and c-axis. Open circles and solid triangles are correspond to $K_\perp$ (θ=90°) and $K_\parallel$ (θ=0°), respectively.

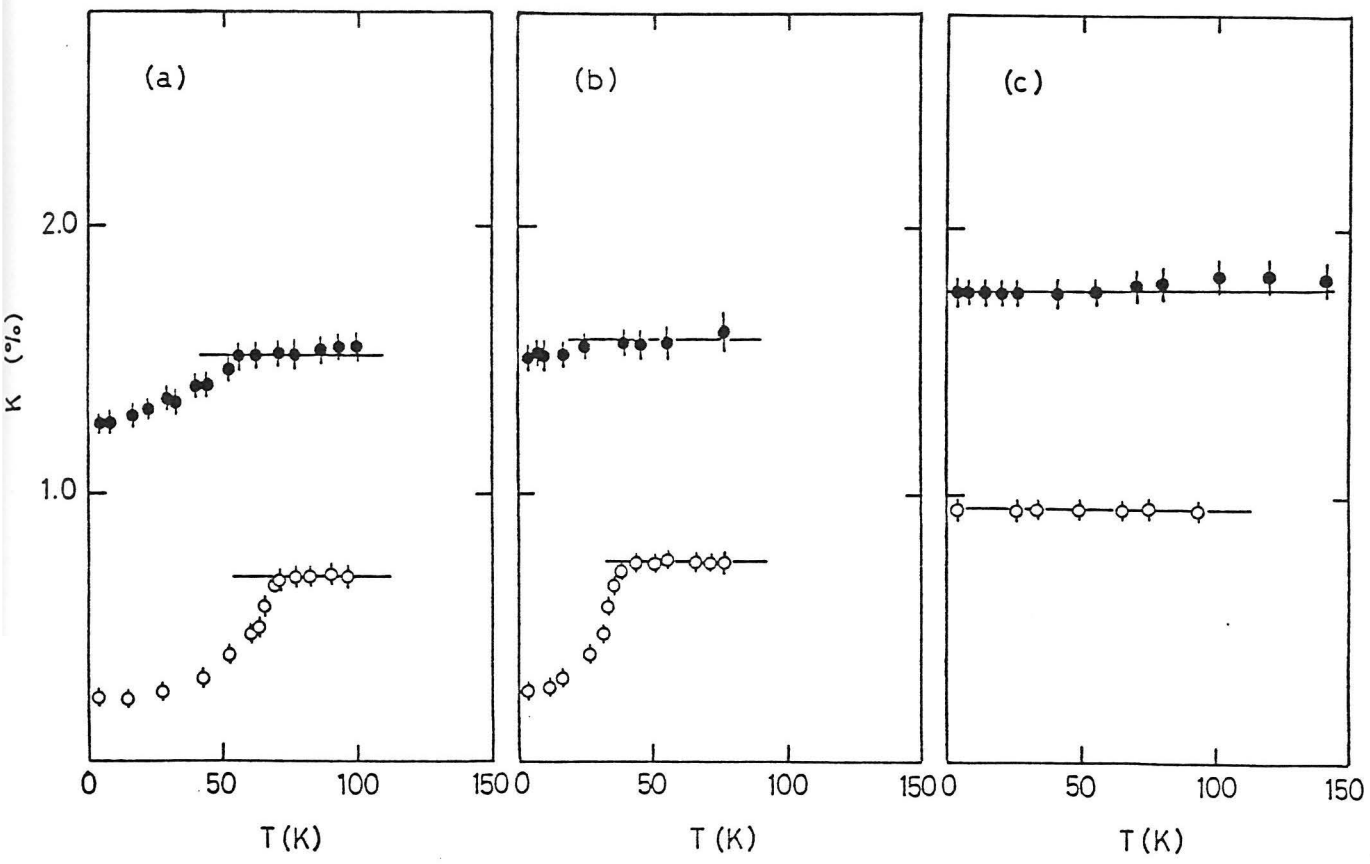

Fig.15. $K_{\perp}$ and $K_{\parallel}$ for the compounds with T_c=72K, 40K and 0 K are shown as closed and open circles in Fig.17 (a)-(c), respectively.

The spin part of $K_{\perp}$ and $K_{\parallel}$ are exclusively coupled to $\chi_s(T)$ by the formula[13),14)]

$$K_{\perp}(T) = A_{\perp}\chi_s(T) + K_{\perp\,orb.}, \quad (1)$$

$$K_{\parallel}(T) = A_{\parallel}\chi_s(T) + K_{\parallel\,orb.}, \quad (2)$$

where K_{orb} is the orbital shift and generally T-independent. The results in $YBa_2Cu_3O_7$ were analyzed by assuming $K_{spin}(T)=0$ at T=0 and $K_{orb}=0.28$ %.[14),15)] In the superconducting vortex state, the screening diamagnetic current produces an additional local field at all nuclear sites. This diamagnetic correction to the shift at 11.5 T is estimated to be less than -0.01 % by assuming the same value as in $YBa_2Cu_3O_7$ obtained at lowest temperature and 7.5T.[14),15)] With these assumptions, $K_{\perp\,orb}$ for $Tl_2Ba_2CuO_{6+y}$ with T_c=72 K and 40 K are evaluated to be 0.24 % and 0.26 %, respectively. The T-dependence of $K_{\perp}$ is similar to that of $YBa_2Cu_3O_7$ reported previously.[14),15)] Namely, above T_c, $K_{\perp}$ is almost T-independent, while below T_c, decreases rapidly. $K_{\perp}$ for the non-superconducting compound is T-independent with a larger value of $K_{\perp}$ =0.95 %. Different from the Curie like behavior of the bulk susceptibility[6)], $\chi_s(T)$ is T-independent in the normal state for $Tl_2Ba_2CuO_{6+y}$. If $K_{\perp orb}$ for the non-superconducting material is assumed to be almost the same as in the superconducting compounds, the magnitude of the spin susceptibility, $\chi_s(T)$ appears to increase with decreasing T_c, in other word, increasing hole concentration.

On the other hand, for the superconducting samples with T_c=72 K and 40 K, both Tc's estimated from the results of $K_{\parallel}$ drop sharply down to 55 K and 20 K, respectively, by the magnetic field. This is consitent with the fact that the magnetic field along the c-axis has a great effect on T_c in the high Tc superconductor. Apparently, it is found that $K_{\parallel}$ also contains spin contributions, which is quite different to the result ($K_{\parallel}$ spin=0) in $YBa_2Cu_3O_7$.[14),15)] Since the value of $K_{\parallel\ orb}$ (=1.27%) for 72 K compound is almost same as that(=1.28%) in $YBa_2Cu_3O_7$[14),15)], $K_{\parallel\ orb}$ is assumed as constant independent of T_c. Then rough estimations of spin susceptibility for respective samples are made by using the same analysis as above. Table 1 shows the spin and orbital contribution to K in each sample.

Table 1. Spin and orbital contribution to K

	$K_{s\perp}$ (%)	$K_{\perp\ orb}$(%)	$K_{s\parallel}$ (%)	$K_{\parallel\ orb}$(%)
T_c=72 K	0.45	0.24	0.25	1.27
T_c=40 K	0.49	0.26	0.30	1.28
T_c= 0 K	0.69	0.26	0.49	1.28
$YBa_2Cu_3O_7$	0.30	0.28	$\sim$ 0	1.28

To argue the spin susceptibility below T_c, the normalized spin susceptibility $\chi_s/\chi_n=(K_\perp-K_{\perp orb})_s/(K_\perp-K_{\perp orb})_n$ deduced from eq. (1) is indicated in Fig. 16 for the compounds with T_c=72 K (solid circles) and 40 K(open circles). As seen in the figure, both appear to show the almost same T-dependence. It should be noted that this T-dependence is quite similar to that for the CuO_2 plane of $YBa_2Cu_3O_7$.[14),15)] When the data of Fig. 18 are tentatively fitted to a calculation based on an isotropic gap model(s-wave) with a larger energy gap of $2\Delta=4.4k_BT_c$ than the BCS value of $3.5k_BT_c$, which is indicated by solid line in Fig. 18, the experiment and the calculation are in good agreement to each other.

On the other hand, if a d-wave model is assumed with a gap zeros of line ($\Delta=\Delta_0\cos\theta$) on the Fermi surface and a large energy gap of $2\Delta_0=10.5k_BT_c$, which explain the Cu relaxation result just below T_c, there is a distinct discrepancy in low temperature as indicated by a dashed line in Fig. 18. Furthermore, the T-dependence of $\chi_s(T)$ extracted from ^{17}O Knight shift for CuO_2 plane in $YBa_2Cu_3O_7$ has also been shown to be well fitted by a s-wave model with $2\Delta=4.9k_BT_c$. Thus the Knight shift results in the CuO_2 plane are consistently interpreted by the s-wave model with a larger energy gap than the BCS value.

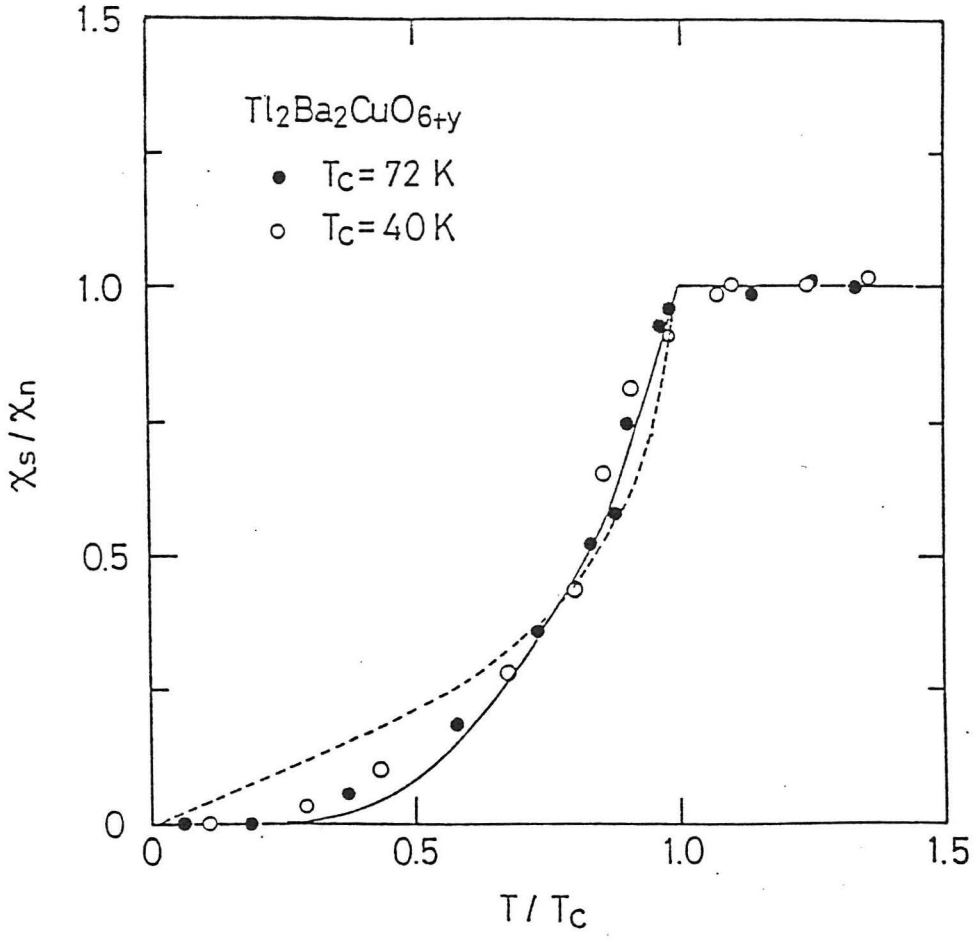

Fig.16. Temperature dependence of the normalized spin susceptibility χ_s/χ_n below T_C deduced from K_{ab} of ^{63}Cu (see text) for $Tl_2Ba_2CuO_{6+y}$ with T_C=72 K (solid circles) and T_C=40 K (open circles). Solid line corresponds to a calculation based on the s-wave model with a larger energy gap of $2\Delta = 4.4k_BT_C$ than the BCS value of $2\Delta = 3.5k_BT_C$. Dashed line indicates a calculation based on a d-wave model with a larger energy gap of $2\Delta_0 = 10.5k_BT_C$ and gap zeros of line on the Fermi surface ($\Delta = \Delta_0 \cos\theta$).

5-2. $1/T_1$ of ^{63}Cu in the High Field NMR

$1/T_1$ of ^{63}Cu in fields perpendicular and parallel to the c-axis were measured by observing (1/2 - -1/2) transition in the NMR spectrum splitted by electric quadrupole interaction.

(1) Temperature Dependence of $1/T_1(\perp)$

$1/T_1(\perp)$ for each sample was measured between 4.2 K and 210 K under a high magnetic field (about 11T) at 125.02MHz. For all samples, the recovery curves are quite well fitted to eq.(1) in chapter 4, as seen in Fig. 17.

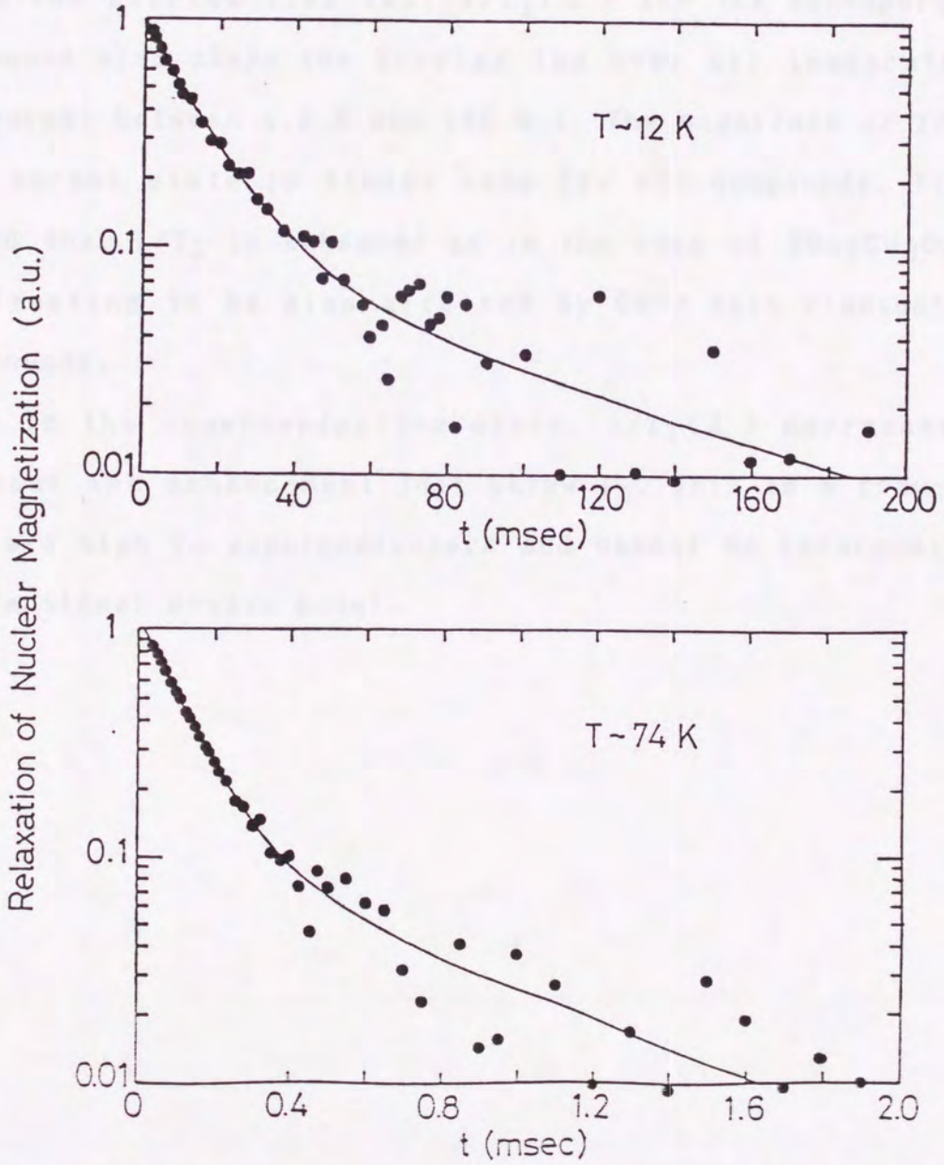

Fig.17. The recovery curve of the nuclear magnetization with the fit to the eq.(4.1) for compounds with T_c=72K at 12K and 74K.

Fig. 18 and 19 show the temperature dependence of $1/T_1(\perp)$ and $(T_1T)_\perp^{-1}$, respectively. Remarkably, $1/T_1(\perp)$ for the superconducting samples obey the $T_1 \cdot T$=const. law , in the wide temperature range above T_c, which is in contrast to the results in $YBa_2Cu_3O_7$[16)-18)], $(La_{1-x}Sr_x)_2CuO_4$ (x=0.075)[19)],etc.. This is the first observation of the Korriga like law of Cu in CuO_2 plane. However, at higher temperture, $1/T_1(\perp)$ deviates gradually from the Korriga like law. $1/T_1(\perp)$ for the nonsuperconducting compound also obeys the Korriga law over all temperature range measured(between 4.2 K and 130 K). The magnitude of $1/T_1(\perp)$ in the normal state is almost same for all compounds. It shoud be noted that $1/T_1$ is enhanced as in the case of $YBa_2Cu_3O_7$[16)-18)], manifesting to be also affected by Cu-d spin fluctuation in Tl compounds.

In the superconducting state, $1/T_1(\perp)$ decreases rapidly without the enhancement just below T_c. This is a common feature for all high Tc superconductors and cannot be interpreted by the conventional s-wave model.

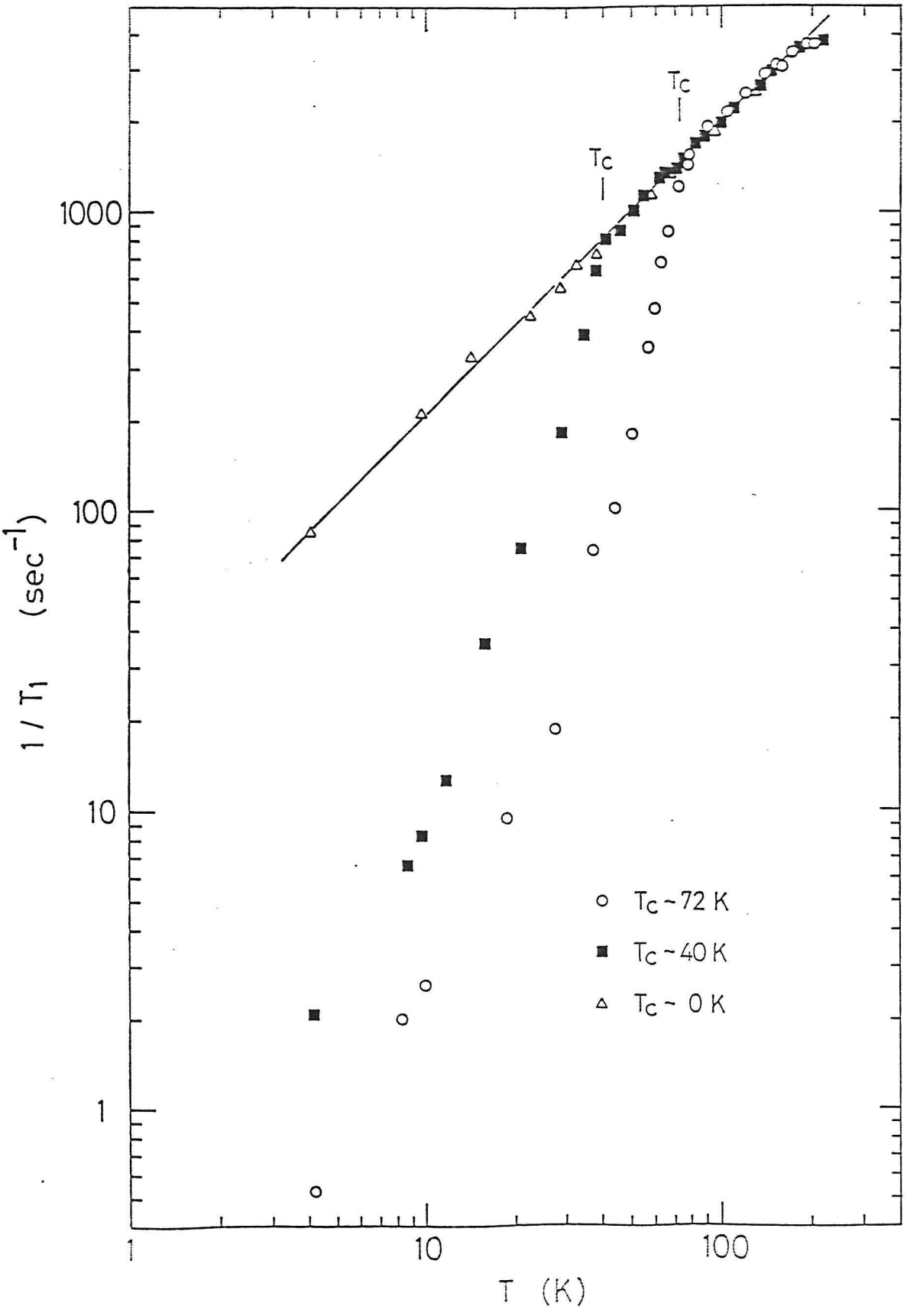

Fig.18. The temperature dependence of $1/T_1$ for ^{63}Cu in $Tl_2Ba_2CuO_{6+y}$. Open circles, solid squares and open triangles indicate the data for compounds with T_c=72K, 40K and 0K, respectively.

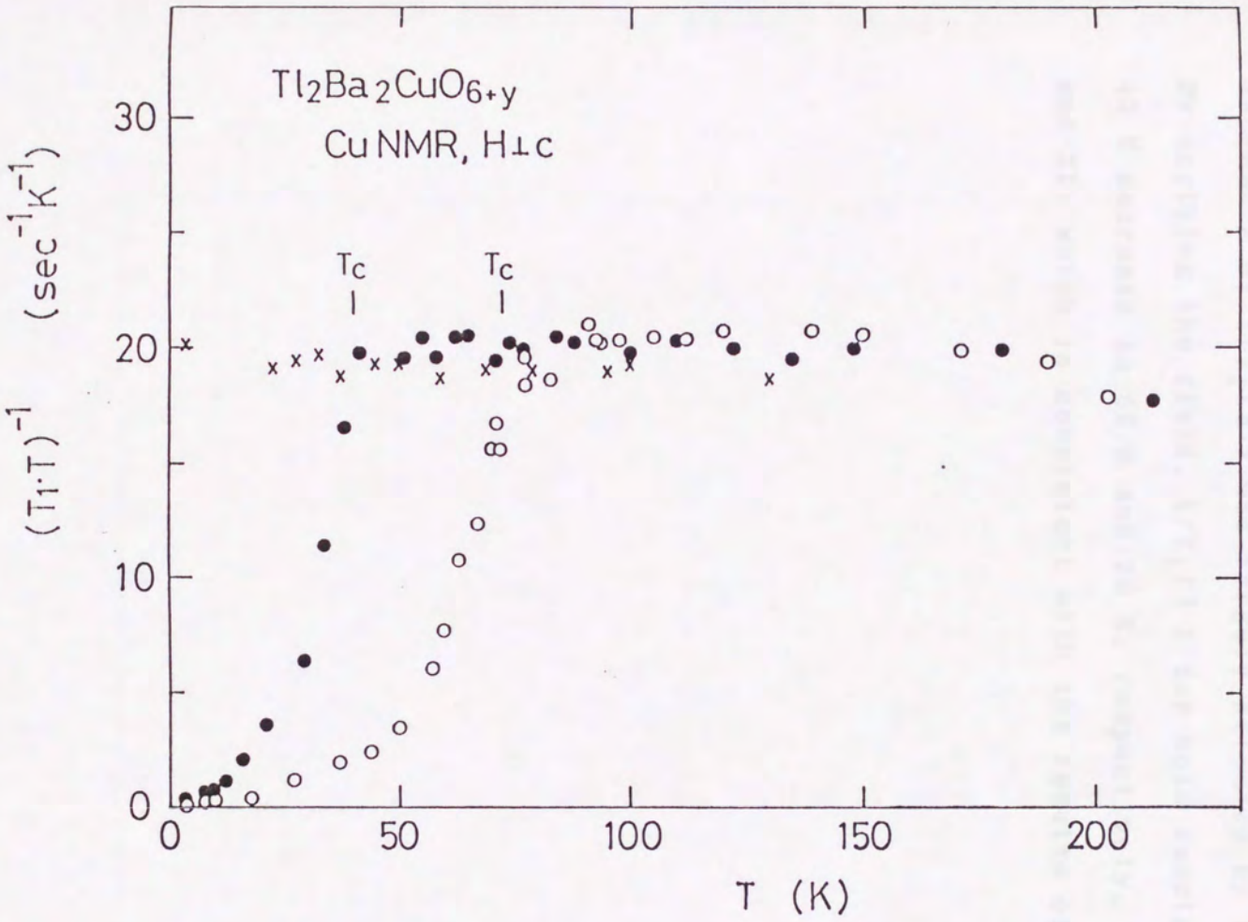

Fig.19. The temperature dependence of $1/(T_1T)$ for ^{63}Cu in $Tl_2Ba_2CuO_{6+y}$. Open circles, solid circles and cross marks indicate the data for compounds with T_c=72K, 40K and 0 K, respectively.

(2) Temperature Dependence of $1/T_1(\parallel)$

It was hard to measure $1/T_1(\parallel)$ precisely at high temperature, since the orientation was not perfect and NMR spin echo signal was weak. However, it was found that the temperature depedence of $1/T_1(\parallel)$ was largely affected by the magnetic field. By applying the field, $1/T_1(\parallel)$ for both samples with T_c=72 K and 40 K decrease to 55 K and 20 K, respectively, as seen in Fig. 20 and 21, which is consistent with the results of $K_\parallel$.

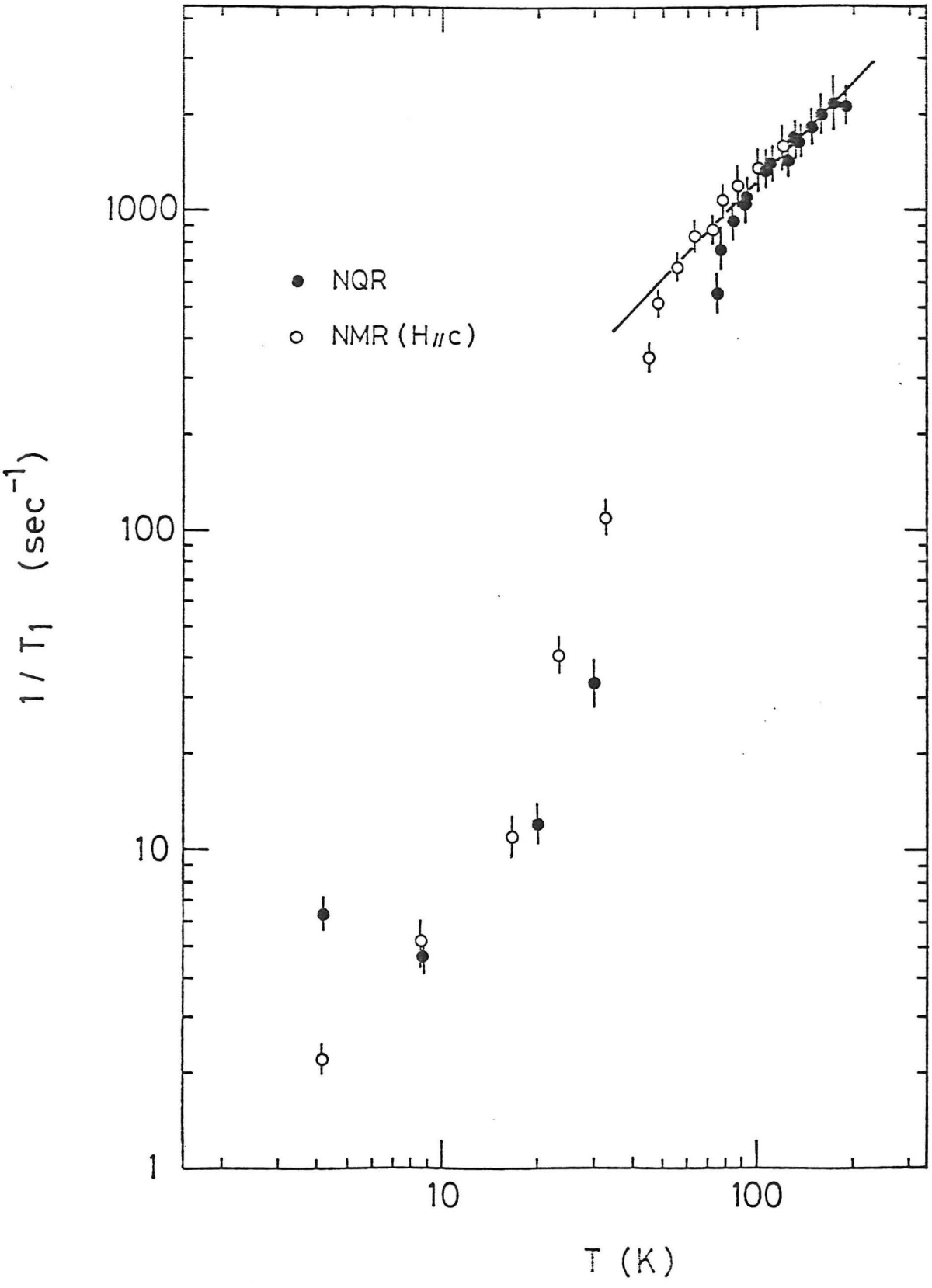

Fig.20. The temperature dependence of $1/T_{1\parallel}$ for ^{63}Cu in the compound with T_c=72K. Open and solid circles indicate the data measured by the high field NMR and the zero field NQR, respectively.

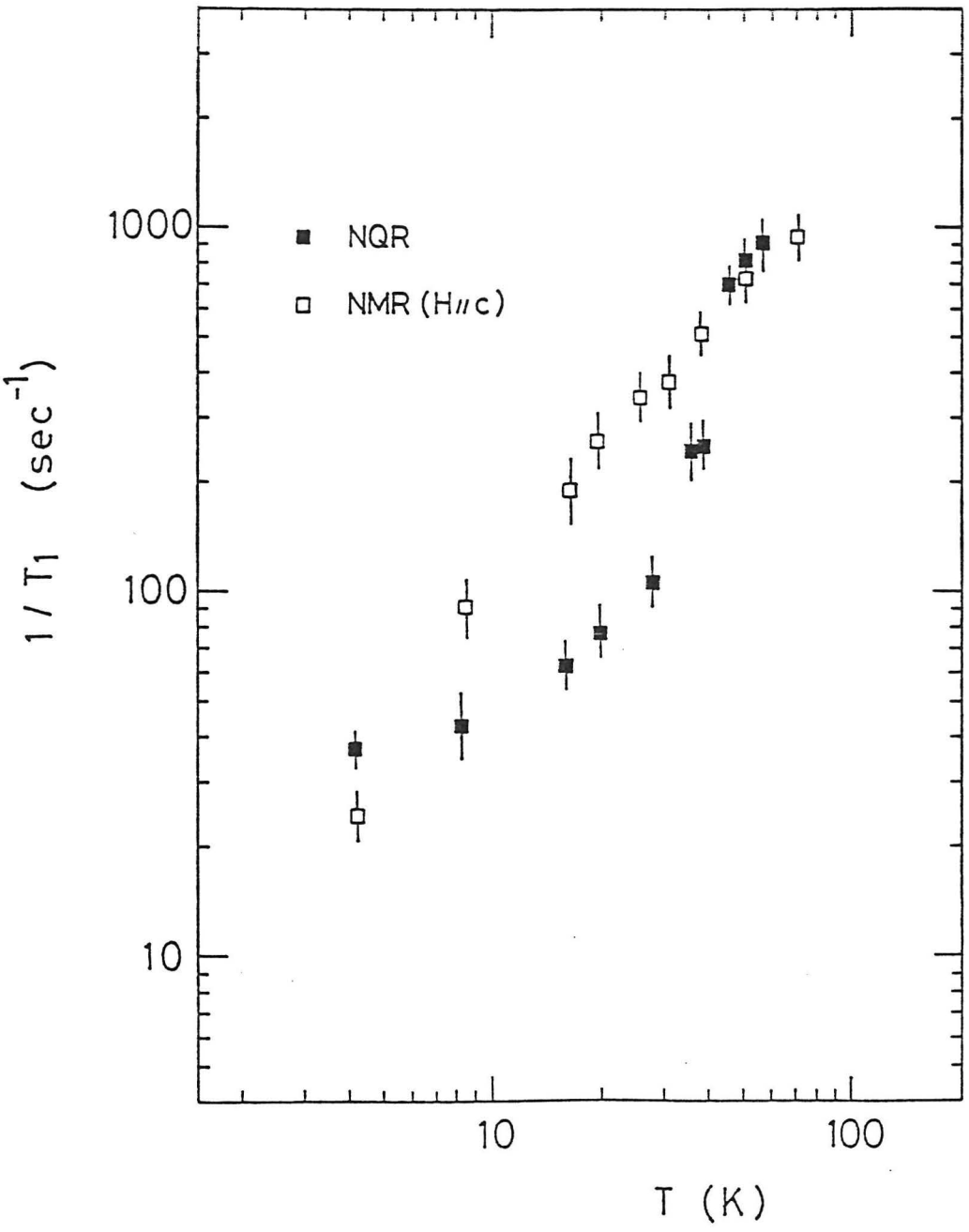

Fig.21. The temperature dependence of $1/T_{1\parallel}$ for ^{63}Cu in the compound with T_c=40K. Open and solid squares indicate the data measured by the high field NMR and the zero field NQR, respectively.

5-3. $1/T_1$ of ^{63}Cu by NQR

Cu NQR spectrum for each compound has been measured by sweeping frequency in the zero external field. Figure 22 shows the spectrum at 4.2 K. As seen in the Fig. 22 , ^{63}Cu and ^{65}Cu line overlap each other because of the broad line width. There is a tendency that NQR line width for the compound with lower T_c is more broader. This tendency may be due to some inhomgeneity owing to the introduced excess oxygens. The peak frequency of ^{63}Cu line for the compounds with T_c=72 K, 40 K, and 0 K were roughly estimated as 22.2MHz, 23.8MHz, and 26.2MHz, respectively. These values are nearly equal to those estimated from the quadrupolar shift, namely, 21.5MHz, 23.8MHz and 26.9MHz.

$1/T_1$'s of ^{63}Cu for all compounds have been measured at each peak frequency. As the principal axis of the electric field gradient is the c-axis, $1/T_1$ measured by NQR gives information along c-axis. The signal-to-noise ratio at 4.2 K is about 3. Figure 23 shows the temperature dependence of $1/T_1$. The behavior of $1/T_1$ is similar to that of $1/T_1(\perp)$. But the magnitude of $1/T_1$ above T_c for superconducting compounds is different from that of $1/T_1(\perp)$, and this difference results from anisotropy of T_1. For nonsuperconducting compound, the magnitude of $1/T_1$ is equal to that of $1/T_1(\perp)$, as seen in Fig. 24.

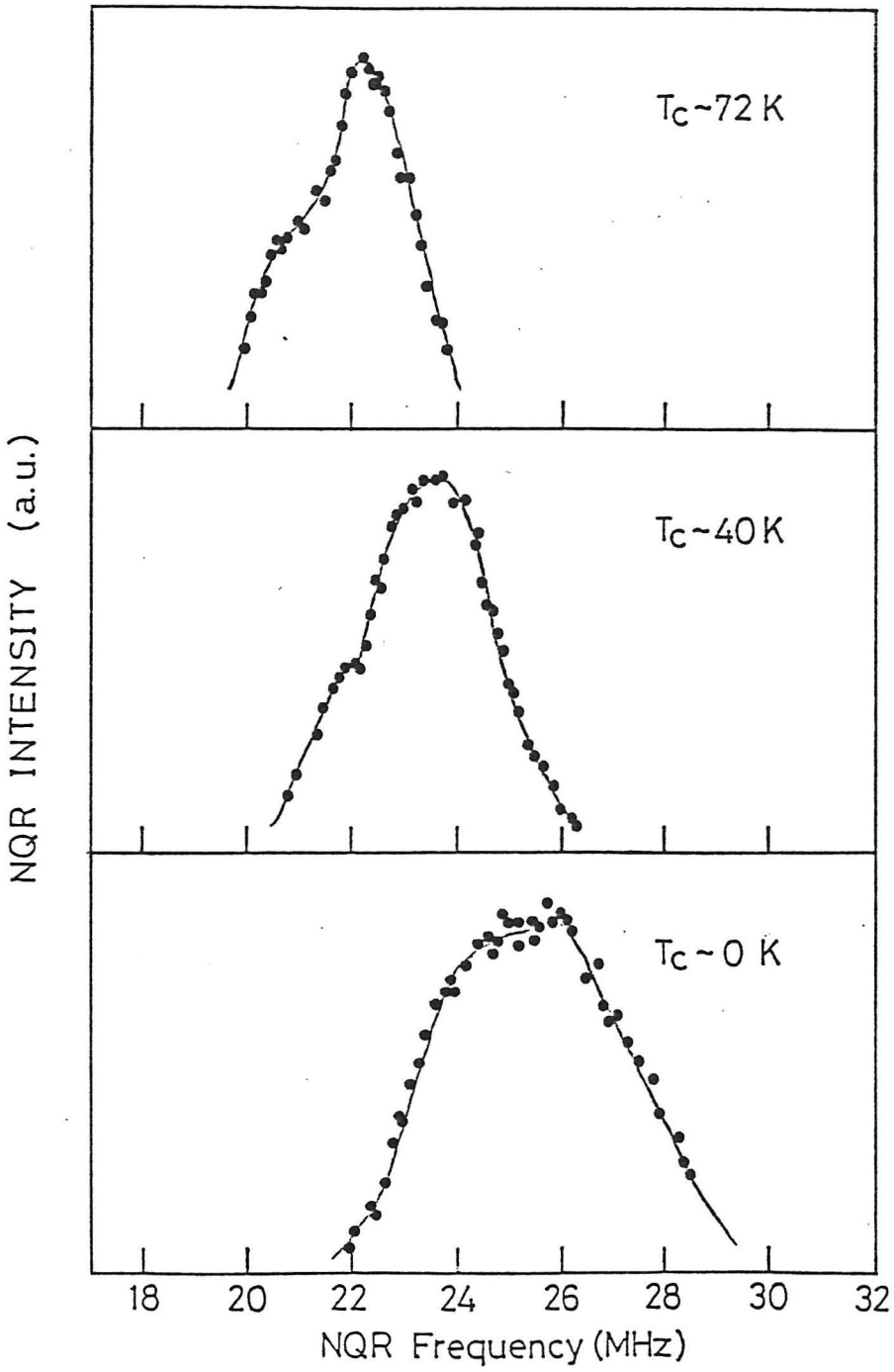

Fig.22. ^{63}Cu, ^{65}Cu NQR spectrum in $Tl_2Ba_2CuO_{6+y}$ at 4.2 K in the zero field.

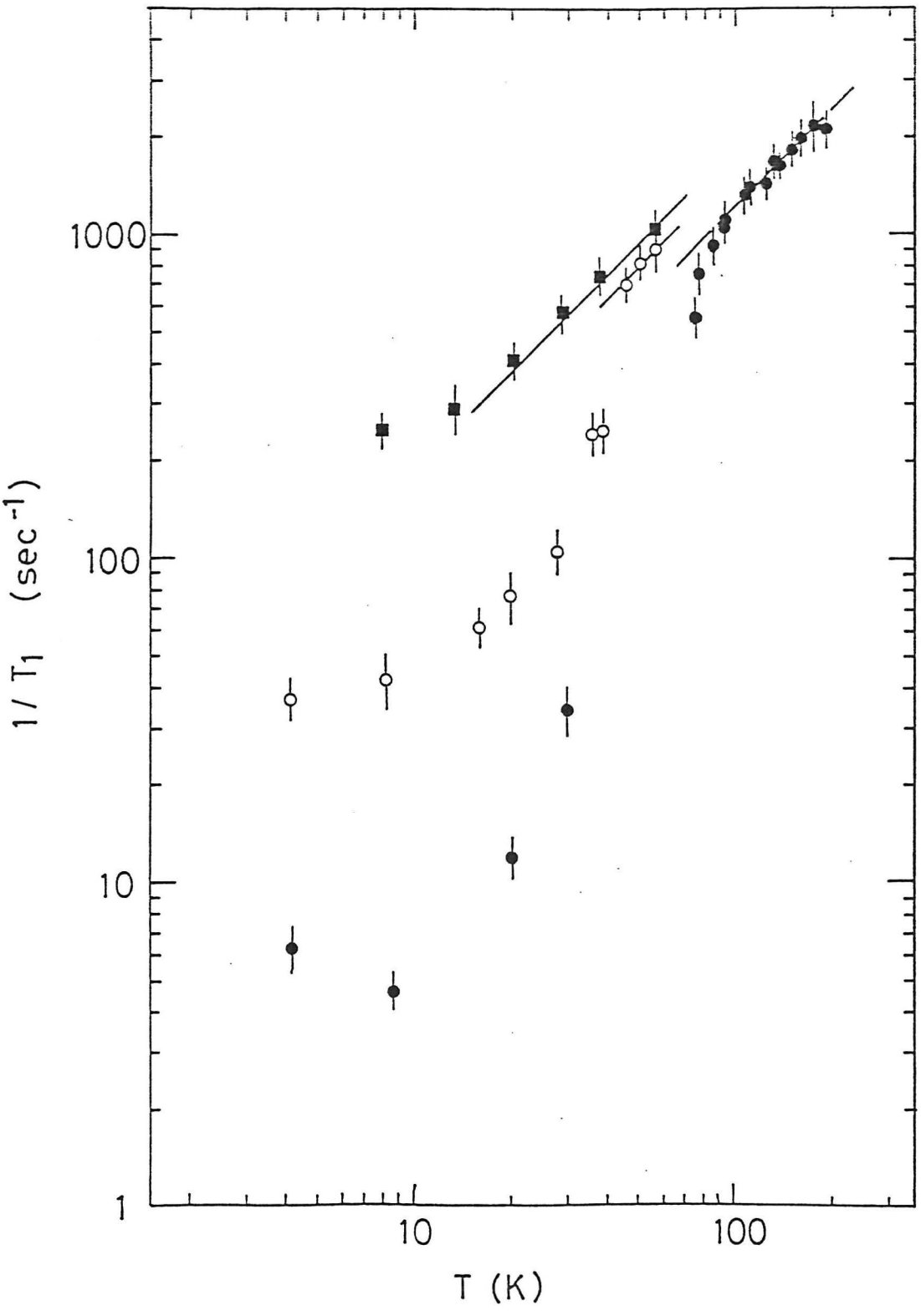

Fig.23. The temperature dependence of $1/T_1$ for ^{63}Cu measured by the zero field NQR in $Tl_2Ba_2CuO_{6+y}$. Solid and open circles and solid squares indicate the data for compounds with T_c=72K , 40K and 0 K, respectively.

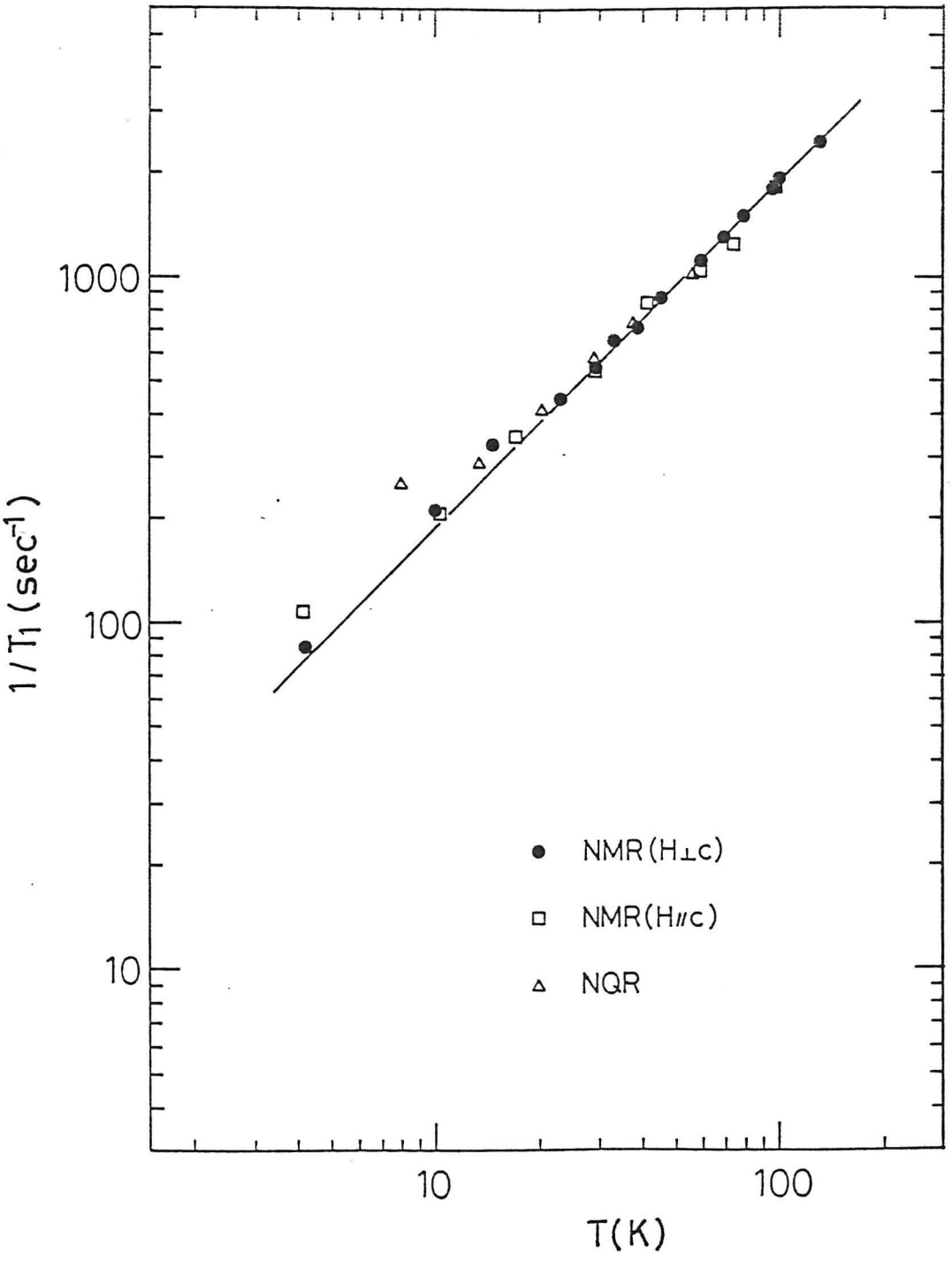

Fig.24. The temperature dependence of $1/T_{1\parallel}$ and $1/T_1$ for ^{63}Cu in the compound with T_c=0 K. Open squares and triangles indicate the data of $1/T_1$ measured by the high field (H∥c) NMR and the zero field NQR, respectively. Solid circles indicate the data of $1/T_1$ measured by the high field (H⊥c) NMR.

5-4. $1/T_1$ of ^{205}Tl in the High Field NMR

The T_1 has been measured along the direction pependicular to the c-axis between 4.2 K and 293 K at 240 MHz. Since ^{205}Tl has no quadrupole moment, T_1 is measured precisely. Actually, above T_c, the recovery curve of the nuclear magnetization was fitted to a single exponential function, as seen in Fig. 25. As NMR spectrum is very sharp, the signal-to-noise ratio is enough to measure T_1 precisely up to nearly 300 K. Figure 26 shows the temperature dependence of $(T_1T)^{-1}$. The behavior of T_1 of ^{205}Tl is similar to that of T_1 of ^{63}Cu. The temperature, T^*, which begin to deviate from Korriga law, was estimated for each sample with T_c= 72 K, 40 K, and 0 K, to be about 150 K, 160 K, and 200 K, respectively.

It is confirmed that $1/T_1$ of ^{205}Tl and ^{63}Cu for the compound with T_c=72 K scale to each other above T_c. Figure 27 shows $1/T_1$ of ^{63}Cu plotted against $1/T_1$ of ^{205}Tl between 80 K and 203 K with temperature as an implicit parameter. The ratio of $^{205}(T_1)/^{63}(T_1)$ is constant above T_c, suggesting that the origin of the relaxation is the same in both Cu and Tl sites. Therefore the relaxation behavior of Cu site is obtained indirectly from that of Tl site.

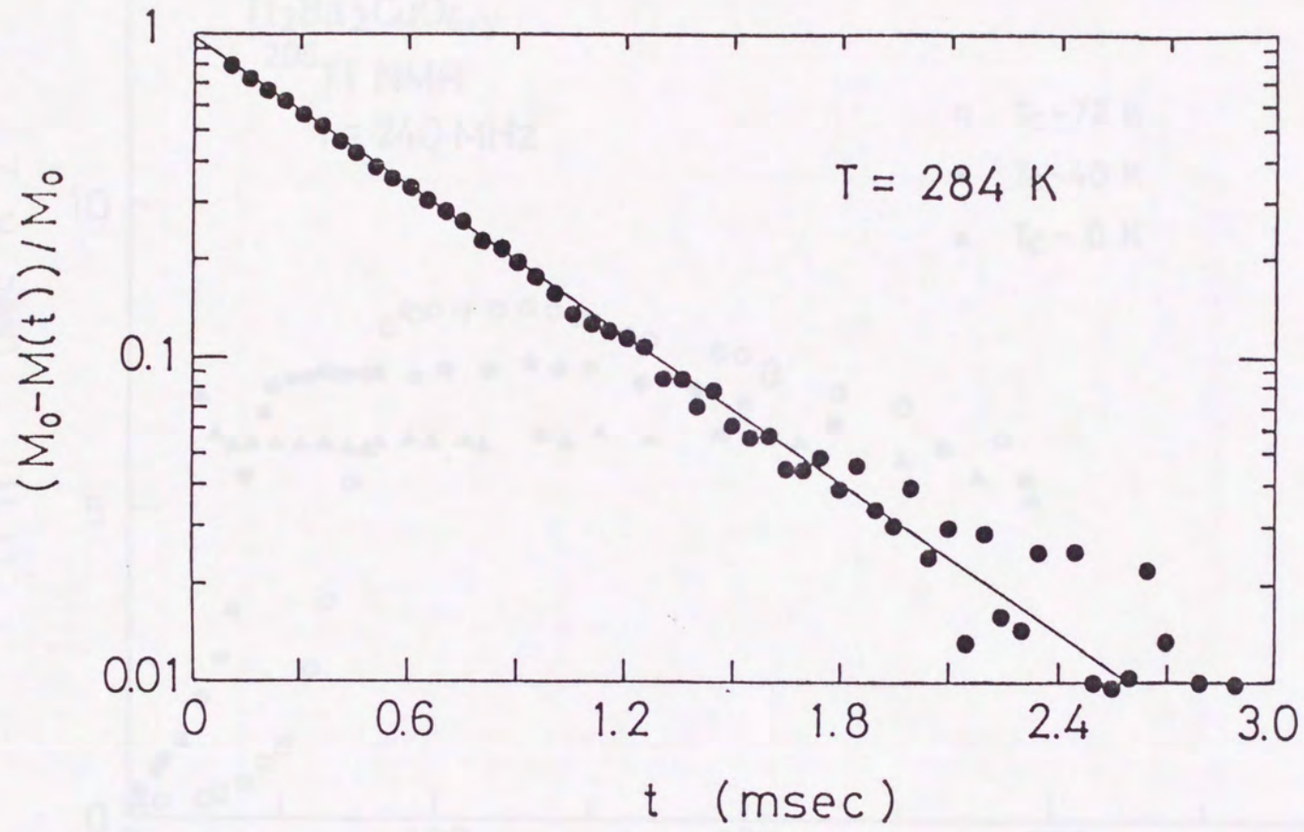

Fig.25. The recovery curve of the nuclear magnetization with the fit to a single exponential function for the compound with T_c=72 K at 284 K.

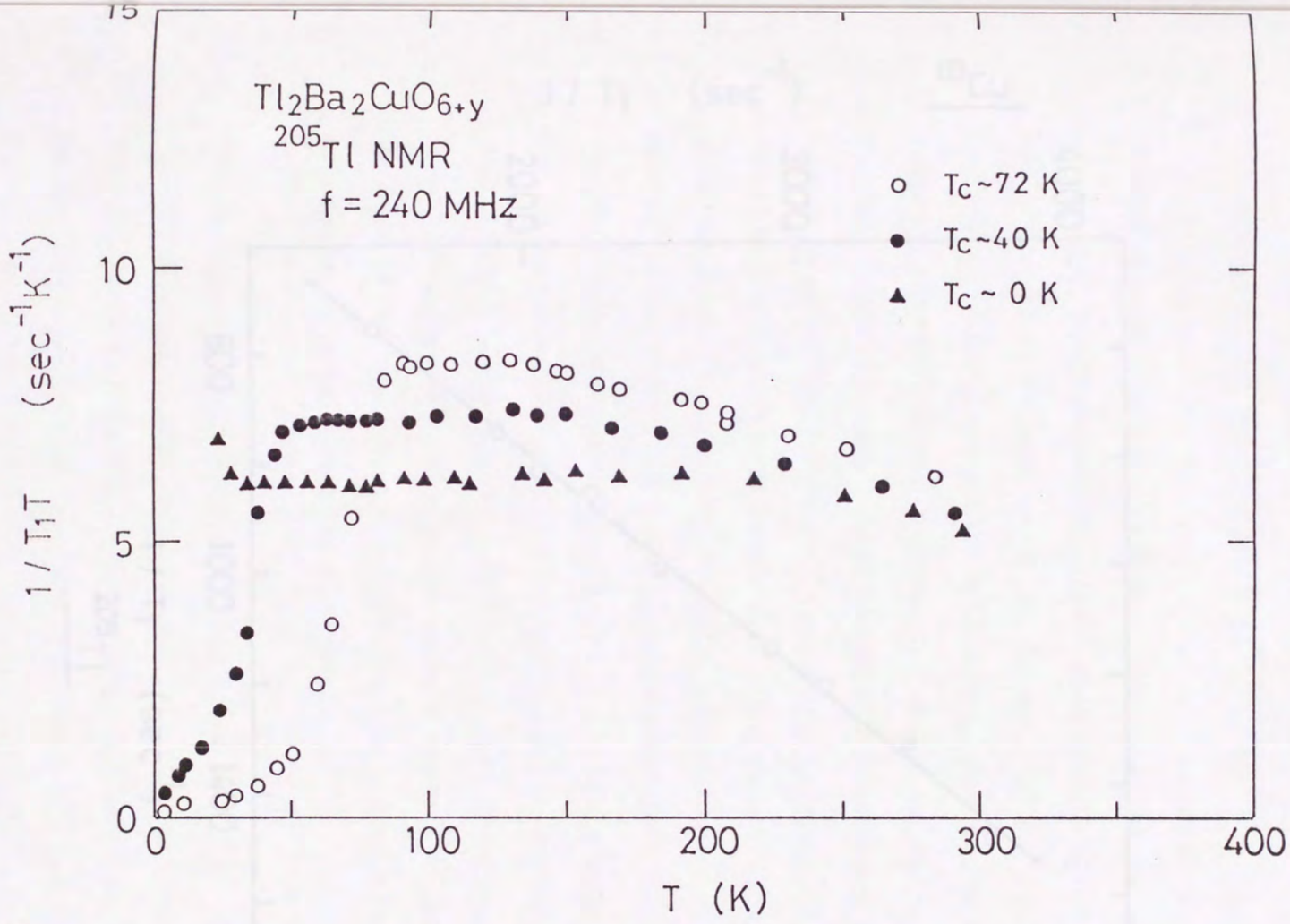

Fig.26. The temperature dependence of $1/(T_1T)$ for ^{205}Tl in $Tl_2Ba_2CuO_{6+y}$. Open and solid circles and solid triangles indicate the data for compounds with T_c=72K, 40K and 0 K, respectively.

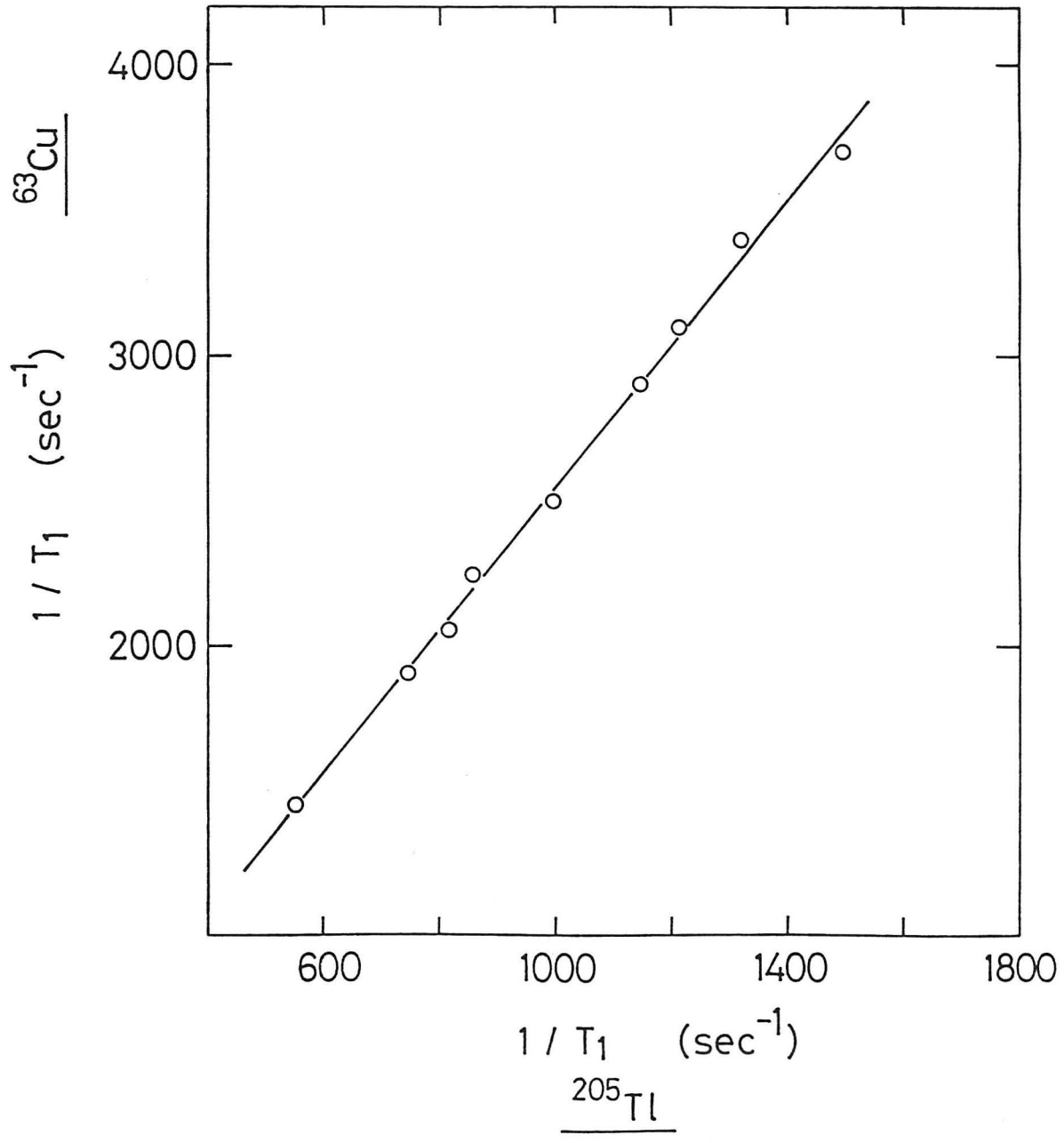

Fig.27. $1/T_1$ of ^{63}Cu are plotted against $1/T_1$ of ^{205}Tl between 80 K and 203 K with temperature as an implicit parameter.

Chapter 6. Discussion

6-1. Normal State

(1) Evidence for Fermi liquid excitation

$1/T_1$'s of ^{63}Cu and ^{205}Tl for all compounds obey T_1T=const. law in a wide temperature range. Applying the high magnetic field along c-axis in superconducting compounds (T_c=72 and 40 K), T_c's decrease from 72 and 40 K to 55 and 20 K, respectively. Then $1/T_1$'s of ^{63}Cu also obey T_1T=const. law above 55 and 20 K. The results support that T_1T=const. law is an intrinsic feature in Tl2201 compound. As the T_1T=const. law means that the energy spectrum of Cu spin excitation is continuous, it is considered that Fermi liquid picture is applicable to Tl2201 compound. Judging from the fact that this series of compounds possess a sufficiently high temperature superconducting transition (=85 K), the a Fermi liquid picture may be a suitable approach to describe the normal state property in high T_c superconductor in general.

$1/T_1$'s of ^{63}Cu and ^{205}Tl for all compounds deviate from T_1T=const. law at higher temperature above T^*. This origin seems to be due to the Cu spin fluctuation. The tendency that T^* increases with hole doping was found.

(2) Comparison with YBCO and LSCO systems

In YBCO and LSCO systems, $1/T_1$ of Cu in CuO_2 plane does not obey T_1T=const. law above T_c, and is enhanced by about one order of the magnitude than the band calculation, reflecting the strong Cu spin correlation.[16)-19)] $1/T_1$ is generally given by

$$1/T_1 \propto k_B T \Sigma \chi(q), \qquad (6.1)$$

where $\chi(q)$ is a dynamical spin susceptibility. The behavior of $1/T_1$ for Cu is qualitatively explained by assuming that $\chi(q)$ has a sharp peak around q=Q as seen in Fig. 30 because of the antiferromagnetic correlation between Cu spins, and that $\chi(Q)$ decreases with T-increase.

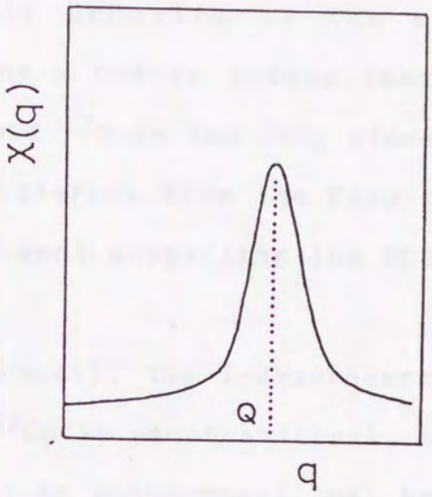

Fig.28. Schematic $\chi(q)$ having a sharp peak at q=Q.

A phenomenological treatment for $1/T_1$ taking account of the Cu-d spin AF correlation has been carried out in YBCO system by several groups.[20)-24)] Recently, Moriya et. al. have extended the self-consistent renormalization theory (SCR theory) of a weakly or nearly AF metal to the two-dimensional system, and predicted that $1/(T_1T) \sim \chi_Q(T)$ and $\chi_Q(T)$ is proportional to $1/(T+\theta)$.[23)]

6-2. Superconducting State

In $Tl_2Ba_2CuO_{6+y}$, the ^{63}Cu Knight shift results below T_c can be well explained in terms of the isotropic gap (s-wave) model if a larger energy gap with $2\Delta = 4.4k_BT_c$ is assumed in contrast to the BCS value of $2\Delta = 3.5k_BT_c$. This behavior of the spin susceptibility below T_c appears to be a rather unique feature when compared to the results of ^{63}Cu and ^{17}O in the CuO_2 plane in $YBa_2Cu_3O_7$.[13)-15),25)] This point is different from the result of the penetration depth by μSR experiment supporting the BCS s-wave model ($2\Delta = 3.5k_BT_c$).[26)]

In contrast to the Knight shift result, the T-dependence of the nuclear relaxation rate, $1/T_1$ of ^{63}Cu is unconventional, that is, the $1/T_1$ decreases rapidly without an enhancement just below T_c characteristic of a BCS superconductor. As seen in Fig. 29, the unconventional behavior is also observed for other several high T_c oxides, and all the $1/T_1$'s normalized by the value at $T=T_c$ plotted against T/T_c fall on a single curve in a wide temperature range below T_c. This result suggests that the same mechanism is responsible for the relaxation process. There may be an alternative explanation for T_1 within the flamework of the s-wave model which involves a pair-breaking effect only near T_c.

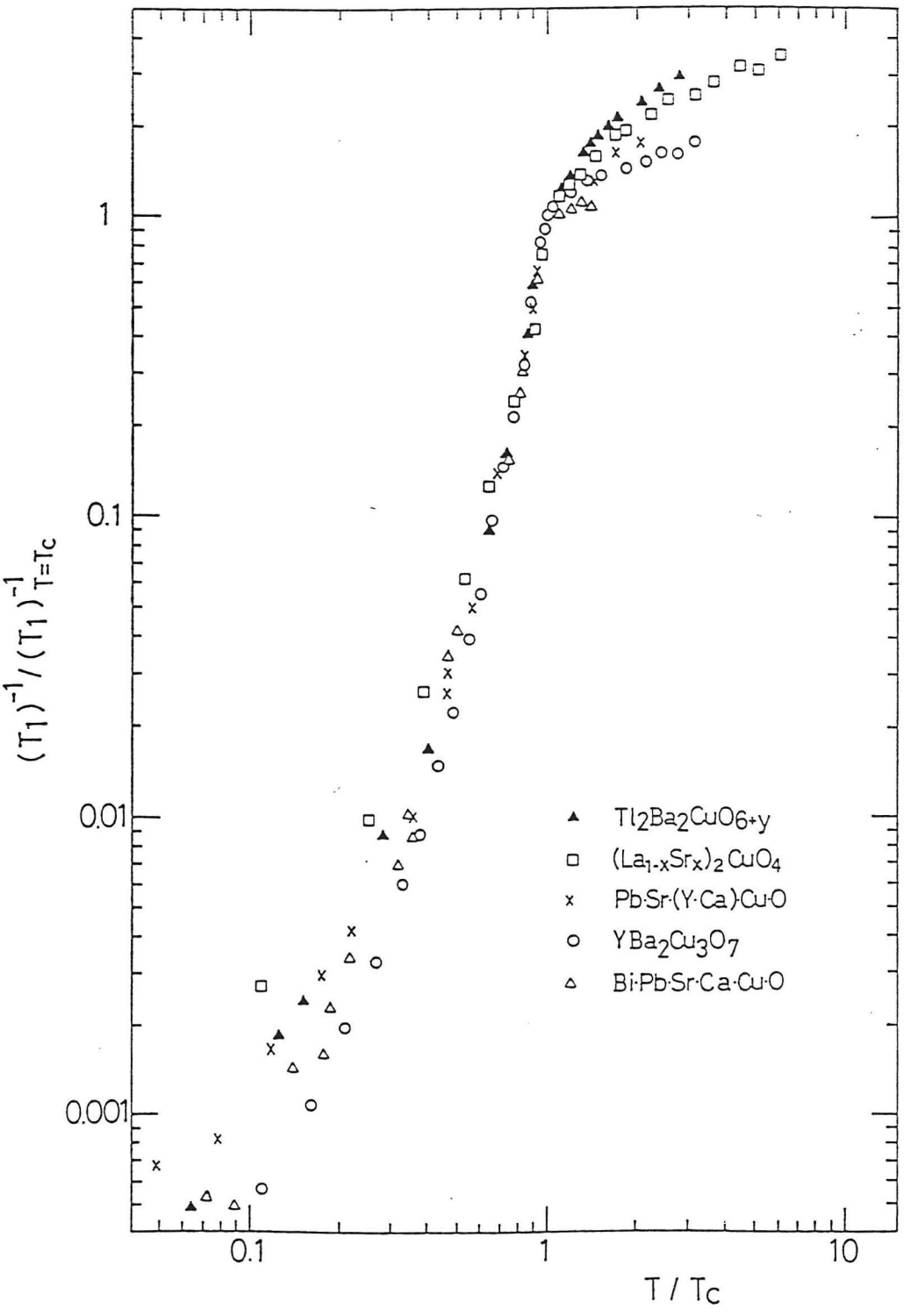

Fig.29. The temperature dependence of $1/(T_1T)$ of ^{63}Cu in the CuO_2 plane sites for $Tl_2Ba_2CuO_{6+y}$(T_c= 40 K), $(La_{1-x}Sr_x)_2CuO_4$, (x= 0.075, 0.15), $YBa_2Cu_3O_7$, respectively.

6-3. Anisotropies of Knight shift and $1/T_1$

Figure 30 shows $K_{s\perp}$, $K_{s\parallel}$ and $(T_1)_\parallel/(T_1)_\perp$ of ^{63}Cu plotted against the hole number per Cu in the CuO_2 plane in $Tl_2Ba_2CuO_{6+y}$, $YBa_2Cu_3O_7$ and $La_{1.85}Sr_{0.15}CuO_4$. Here K_s is a spin contribution to the Knight shift. In Tl2201, as the hole number increases, both $K_{s\perp}$ and $K_{s\parallel}$ increase and $(T_1)_\parallel/(T_1)_\perp$ approaches 1 gradually, that is, the anisotropies of K_s and T_1 become small. It is well known that the origin of the anisotropy is due to the anisotropy of the hyperfine coupling constant. In the high T_c superconductors, $K_{s\perp}$ and $K_{s\parallel}$ of Cu in the CuO_2 plane are generally given by

$$K_{s\perp} = A_\perp \chi_s = (A_{ab} + 4B)\chi_s,$$

$$K_{s\parallel} = A_\parallel \chi_s = (A_c + 4B)\chi_s.$$

Here A_{ab} and A_c are components perpendicular and parallel to c-axis of an on-site hyperfine coupling constant. B is an isotropic term resulting from supertransferred hyperfine interaction between nearest neighbor Cu sites. Unfortunately, in Tl2201, since both K_s and χ_s are independent of temperature above T_c, it is impossible to estimate $A_\perp$ and $A_\parallel$.

In $YBa_2Cu_3O_7$, A_{ab}, A_c and B are estimated at 30, -164 and 41kOe/μ_B, respectively. Taking account of the fact that A_{ab} and A_c are not affected by hole doping in YBCO system, we assume that A_{ab} and A_c in Tl2201 are nearly equal to those in $YBa_2Cu_3O_7$. Then it is considered that both $K_\perp$ and $K_\parallel$ are increased by increase of B term with hole-doping.

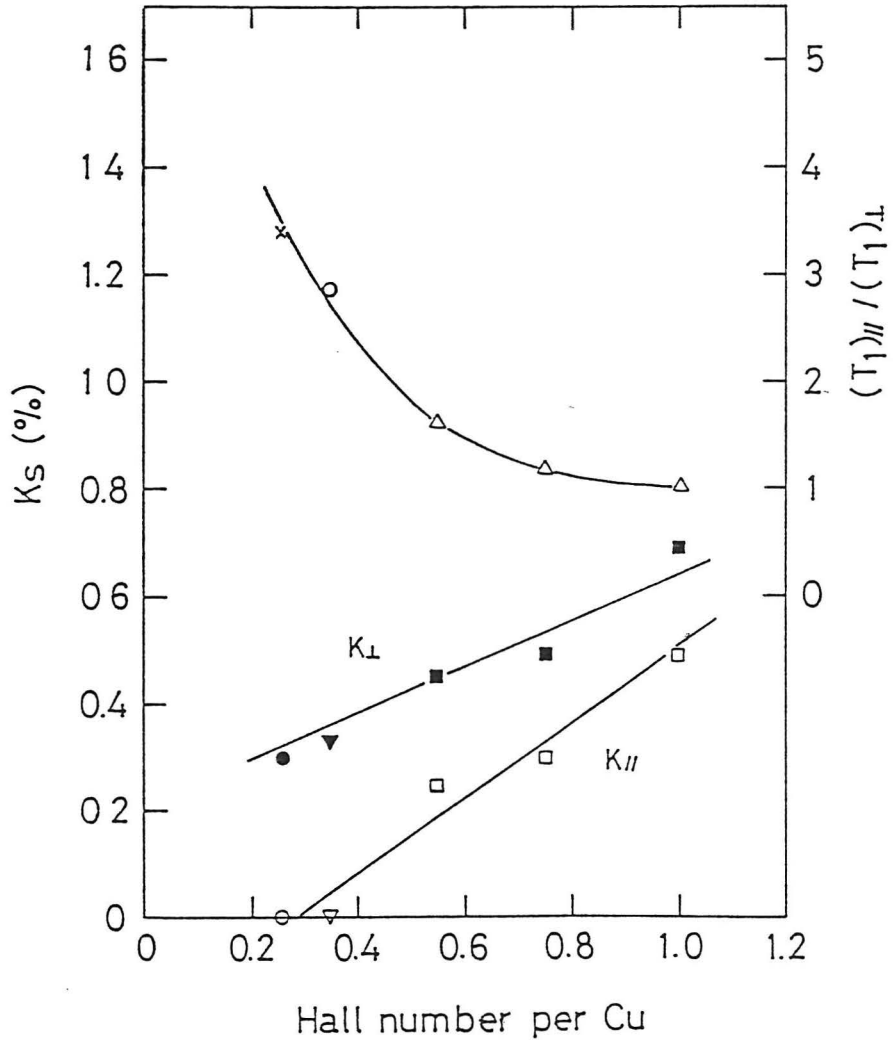

Fig.30. The temperature dependence of $1/T_1$ of ^{63}Cu in the CuO_2 plane sites for $Tl_2Ba_2CuO_{6-y}$(T_c=72K), $La_{1.85}Sr_{0.15}CuO_4$, $YBa_2Cu_3O_7$, Bi·Pb·Sr·Ca·Cu·O and Pb·Sr·(Y·Ca)·Cu·O.

Chapter-7. Summary

By studying about $Tl_2Ba_2CuO_{6+y}$ using NMR technique, "heavy-doped" superconductor was found to possess a characteristic feature. In the normal state, $1/T_1$'s of ^{63}Cu in the CuO_2 plane for all compounds obey Korringa like (T_1T=const.) law in a wide temperature range, suggesting that Fermi liquid picture is applicable to Tl2201 compound. The magnitude of $1/T_1$ does not change with hole concentration, in contrast to the result that $1/T_1$ of Cu for "light-doped" La-Sr-Cu-O superconductor decreases considerably with increasing holes. This difference may be attributed to the difference of strength of Cu-d spin antiferromagnetic correlation between "heavy-doped" and "light-doped" superconductors.

In superconducting state, the temperature dependence of the susceptibility is explaned by BCS model with a larger gap of $2\Delta = 4.4k_BT_c$ than the BCS value of $2\Delta = 3.5k_BT_c$. However $1/T_1$ of ^{63}Cu is unconvetional and decreases rapidly without the enhancement just below T_c predicted by the BCS model. The unconventional behavior is commonly observed in other several high T_c superconductors.

Acknowledgements

The author would like to express his sincere thanks to Professor Kunisuke Asayama for guiding him into this field, and for the continuous advice, enlighting discussions and warm-hearted encouragement throughout this work. He would like to thank Associated Professor Yoshio Kitaoka for continuous guidance, valuable discussions and encouragement. He also thanks Profesor Y. Oda and Associated Profesor Yoh Kohori for numerous advices, Dr's Y. Shimakawa, T. Manako, Y.Kubo and H.Igarashi for thier material syntheses and characterizations, and the colleagues in our laboratory for many helps.

References

1) J.G.Bednortz and K.A.Muller: Z. Phys. B64 (1986) 189.

2) K.Asayama and Y.Kitaoka: Solid State Phys. vol.23 No.6 (1988) 353.

3) Y.Shimakawa, Y.Kubo, T.Manako, T.Satoh, S.Iijima, T.Ichihashi and H.Igarashi: Physica C157 (1989) 279.

4) Y.Shimakawa, Y.Kubo, T.Manako and H.Igarashi: Phys. Rev. B40 (1989) 11400.

5) Y.Shimakawa, Y.Kubo, T.Manako, H.Igarashi, F.Izumi and H.Asano: submitted to Phys. Rev. B.

6) Y.Kubo, Y.Shimakawa, T.Manako, and H.Igarashi: submitted to Phys. Rev. B.

7) H.Takagi: Solid State Phys. Vol.25 No.10 (1990) 736.

8) K.Yoshida: Phys. Rev. 110 (1958) 769.

9) H.L.Fine, M.Lipsicas and M.Strongin: Phys. Lett. 29A (1969) 366.

10) L.C.Hebel and C.P.Slichter: Phys. Rev. 113 (1957) 1504.

11) Y.Masuda and A.G.Redfield: Phys. Rev. ^{125} (1962) 159.

12) M.Takigawa, P.C.Hammel, R.H.Heffner, Z.Fisk, J.I.Sumith and R.B.Schwartz: Phys. Rev. B39 (1989) 300.

13) Y.Yoshinari, H.Yasuoka, Y.Ueda, K.Koga and K.Kosuge: J. Phys. Soc. Jpn. 59 (1990) 3698.

14) M. Takigawa: Proceeding of the NATO Workshop on the Dynamics of Magnetic Fluctuation in High Temperature superconductors (Plenum Press) to appear.

15) S.E. Barret, D.J. Durand, C.H. Pennington, C.P. Slichter, T.A. Friedmann, J.P. Rice, and D.M. Ginsberg: Phys. Rev. B41 (1990) 6283.

16) R.E.Walstedt, W.W.Warren,Jr., R.F.Bell, G.F.Brennert, G.P.Espinosa, J.P.Remeika, R.J.Cava and E.A.Reitman: Phys. Rev. B36 (1987) 5727.

17) Y.Kitaoka, H.Hiramatsu, T.Kondo and K.Asayama: J. Phys. Soc. Jpn. 57 (1988) 30.

18) T.Imai, T.Simizu, T.Tsuda, H.Yasuoka, T.Takabatake, Y.Nakazawa and M.Ishikawa: J. Phys. Soc. Jpn. 57 (1988) 1771.

19) K.Ishida, Y.Kitaoka and K.Asayama:J. Phys. Soc. Jpn. 58 (1989) 36.

20) B.S.Shastry: Phys. Rev. Lett. 63 (1989) 1288.

21) A.J.Millis, H.Monien, D.Pines: Phys. Rev. B42 (1990) 167.

22) N.Bulet, D.Hone, D.Scarapino and N.E.Bickers: Phys. Rev. B41 (1990) 1797.

23) T.Moriya, T.Takahashi and K.Ueda: J. Phys. Soc. Jpn. 59 (1990) 2905 , Y.Kitaoka, K.Fujiwara, K.Ishida, S.Ohsugi and K.Asayama: Prog. Theor. Phys. Suppl. No.101, 1990, to appear

24) H.Monien, D.Pines and M.Takigawa: Phys. Rev. B in press.

25) K.Ishida et al.: in preparation.

26) D.R.Harshmann et al.: Phys. Rev. B39 (1989) 851.